Pharmacological Research 234 (2026) 109712



Contents lists available at ScienceDirect

Pharmacological Research

journal homepage: www.elsevier.com/locate/yphrs



Striatofugal balance and beneficial effects of facilitating nucleus accumbens mGlu4 receptor activity in the *Fmr1*$^{-/-}$ mouse model of Fragile X Syndrome

Mathieu Fonteneau [a,*,1], Claire Terrier [a,b,1], Florian Bolot [a], Fani Pantouli [b,c,2], Agathe Brugoux [a], Fanny Malhaire [d], Ingrid Wagnon [b,3], Roser Borràs-Tuduri [e], Paola Rossolillo [f], Isabelle McCort-Tranchepain [g], Alexis Bailey [c], Francine Acher [g,4], Amadeu Llebaria [e], Cyril Goudet [d], Jérôme A.J. Becker [a,b,5], Julie Le Merrer [a,b,5]

[a] *Université de Tours, INSERM, Imaging Brain & Neuropsychiatry iBraiN U1253, Tours 37032, France*
[b] *Physiologie de la Reproduction et des Comportements, INRAe UMR-0085, CNRS UMR-7247, IFCE, Université de Tours, Inserm, Nouzilly 37380, France*
[c] *Division of Pharmacology, School of Health & Medical Sciences, City St George's University of London, London SW17 ORE, UK*
[d] *Institut de Génomique Fonctionnelle (IGF), Université de Montpellier, CNRS, Inserm, Montpellier 34094, France*
[e] *MCS, Laboratory of Medicinal Chemistry and Synthesis, Institute of Advanced Chemistry of Catalonia (IQAC-CSIC), Barcelona, Spain*
[f] *Institut de Génétique et de Biologie Moléculaire et Cellulaire (IGBMC), Université de Strasbourg, CNRS UMR 7104, Inserm UMR-S, Illkirch, France*
[g] *Laboratoire de Chimie et Biochimie Pharmacologiques et Toxicologiques, CNRS UMR8601, Université Paris Cité, Paris Cedex 06, 75270, France*

ARTICLE INFO

Keywords:
Autism spectrum disorder
Striatal projection neurons
Nucleus accumbens
Ventral pallidum
Metabotropic glutamate receptor 4
Social behavior

ABSTRACT

Fragile X Syndrome (FXS) is the leading monogenic cause of autism spectrum disorder (ASD). To date, no approved pharmacological treatment alleviates social impairments in patients with FXS. Since D1 and D2 dopamine receptor-expressing striatal projection neurons (SPNs) were shown to regulate ASD-sensitive behaviors, we explored whether the balance of activity between D1- and D2-SPNs would be biased in the *Fmr1*$^{-/-}$ mouse model of FXS. We evaluated striatal function in *Fmr1*$^{-/-}$ and *Fmr1*$^{+/+}$ mice under pharmacological challenge and performed RNAscope® *in situ* hybridization following social interaction to assess the activity of SPNs in the nucleus accumbens (NAc) and dorsal striatum. We evidenced a decrease in D1-SPN activity, biasing the D1/D2-SPN balance. We then evaluated the effects of compounds developed to repress D2-SPN activity on behavioral impairments in *Fmr1*$^{-/-}$ mice. Systemically facilitating mGlu4 or blocking A2a receptor activity relieved behavioral deficits in this model. Moreover, social interaction in *Fmr1*$^{-/-}$ mice was fully rescued by photopharmacological activation of mGlu4 in the ventral pallidum, to which both NAc D1- and D2-SPNs project, and mGlu4 receptors in the NAc likely contributed to restoring social deficits after systemic mGlu4 facilitation. Together, these results are consistent with our working hypotheses of both biased striatal D1/D2-SPN balance in social deficit and contribution of mGlu4 receptors expressed by NAc SPNs in modulating social behavior. In conclusion, pharmacological compounds able to regulate SPN activity demonstrate a promising therapeutic potential to relieve ASD-like deficits in FXS.
Pharmacological compounds: ADX88178 (CAS 1235318–89–4); haloperidol hydrochloride (CAS 1511–16–6); istradefylline (CAS 155270–99–8); LSP4–2022 (CAS 1413405–33–0); morphine hydrochloride (CAS 6055–06–7); quinpirole hydrochloride (CAS 85798–08–9); SCH-23390 hydrochloride (CAS 125941–87–9); SKF-81297 hydrobromide (CAS 67287–39–2); sulpiride (CAS 15676–16–1); VU0155041 sodium (CAS 1259372–69–4); optogluram (CAS 1627840–48–5)

* Corresponding author.
E-mail address: mathieu.fonteneau@univ-tours.fr (M. Fonteneau).
[1] equally contributed to the work
[2] current address: Florida Research & Innovation Center, Cleveland Clinic, 9801 SW Discovery Way, Port St. Lucie, FL, 34987, USA
[3] current address: Department of Natural Science and Environment, Roskilde University, Roskilde, Denmark.
[4] current address: Saints-Peres Paris Institute for the Neurosciences, Université Paris Cité, 75270 Paris Cedex 06, France.
[5] equally contributed to the work

https://doi.org/10.1016/j.phrs.2026.109712

Available online 28 October 2026
1043-6618/© 2026 The Authors. Published by Elsevier Ltd. This is an open access article under the CC BY-NC-ND license (http://creativecommons.org/licenses/by-nc-nd/4.0/).

1. Introduction

Autism spectrum disorders (ASD) are complex neurodevelopmental disorders whose diagnosis is reached in presence of impaired social communication and interaction together with a restricted, repetitive repertoire of behaviors, interests and activities [1]. The etiopathological mechanisms underlying ASD remain essentially unknown, although a clear genetic contribution has been identified [2,3]. Fragile X syndrome (FXS) is the most prevalent monogenic cause of ASD, accounting for 1–6% of total cases [4–6]. FXS results from CGG repeat expansion (>200) in the *Fmr1* gene, impeding the transcription of the Fragile X Messenger Ribonucleoprotein (FMRP). About 50% of males and 20% of females with FXS meet the diagnosis for ASD; other behavioral and neurologic challenges include intellectual disability, generalized anxiety, hyperactivity and epilepsy [4,5,7]. Current treatments target comorbid symptoms such as anxiety, sleep problems or epilepsy [5,8] but fail to relieve cognitive impairment or core social deficits of ASD. Preclinical evidence of cellular and behavioral benefits of mGlu5 inhibitors [9,10] raised major hopes for FXS treatment, but these compounds disappointingly failed in clinical trials [11,12].

Complex neuropsychiatric profile in FXS points towards widespread alterations of the central nervous system. Indeed, as an RNA-binding protein, FMRP regulates the expression of multiple key components of synaptic function throughout the brain [13–15]. The high prevalence of learning disabilities and cognitive deficits in this syndrome have led to an extensive investigation of cortical [16–18] and hippocampal [19,20] dysfunction in this disorder. However, clinical and preclinical evidence for motor impairment, behavioral inflexibility, reward and social deficits in FXS [4,21,22] point towards altered striatal function, as proposed for ASD [23–25]. Within the striatum, the nucleus accumbens (NAc), a hub structure of the reward circuitry [26–28] that plays a unique role in reward processing and goal-directed behavior [26,29], has received little attention in FXS. This region plays a key role in modulating social and repetitive behaviors [30–32], questioning a potential contribution of NAc dysfunction to ASD-like symptoms in FXS.

GABAergic striatal projection neurons (SPNs) represent the main neuronal population in the NAc, and segregate into dopamine D1 receptor (D1) and D2 receptor (D2)-expressing subtypes. A finely tuned balance of activity between D1- and D2-SPNs in the NAc drives approach and avoidance behaviors [33], including towards congeners [31,32,34–37]. Convergent evidence points towards altered NAc physiology in the mouse model of FXS, the *Fmr1*$^{-/-}$ mice. NAc SPNs indeed display altered synaptic plasticity and dendritic morphology in this model [38,39]. The lack of FMRP reshapes the *ex vivo* electrophysiological profile of D1- and D2-SPNs in the NAc Core, favoring D2-SPN intrinsic excitability [40]. Moreover, the functional connectivity of the NAc is modified in a pathway-dependent manner in *Fmr1*$^{-/-}$ mice: the synaptic strength of prefrontal cortex (PFC) and basolateral amygdala (BLA) projections to NAc Core D2-SPNs is increased, together with dendritic spine density of NAc Core D2-SPNs [41]. Given the role of NAc SPNs in controlling social behavior [31,32,36,42], one would consider plausible that biased NAc SPN balance towards an excessive weight of D2-SPN outputs would participate in the ASD-like symptomatology in FXS [24,25,31,32]. In support of this hypothesis, facilitating the activity of the metabotropic glutamate receptor 4 (mGlu4), highly expressed on SPN terminals and known to inhibit GABA release from D2-SPN terminals [43–48], or blocking the adenosine 2A (A2a) receptor, whose expression is highly enriched in D2-SPNs [49,50], were recently found to improve cellular and behavioral features in *Fmr1*$^{-/-}$ mice [51,52].

In the present study, we explored striatal-dependent behaviors in *Fmr1*$^{-/-}$ mice in response to dopaminergic and opioid compounds, in search of functional evidence of a bias in the D1/D2-SPN balance of activity. Using the RNAscope® in situ hybridization (ISH) technique, we evaluated post-mortem the neuronal activity of D1- and D2-SPNs in the ventral (NAc Core and Shell) and dorsal (DS) striatum following a social encounter in *Fmr1*$^{-/-}$ and *Fmr1*$^{+/+}$ mice. Then, we evaluated the therapeutic potential of four compounds developed to decrease D2-SPN activity: two positive allosteric modulators (PAMs: VU0155041 and ADX88178) and an orthosteric agonist (LSP4–2022) of mGlu4, as well as an A2a antagonist, istradefylline [43,46–48,50,53–56]. We examined their ability to alleviate ASD-like symptoms in *Fmr1*$^{-/-}$ mice after systemic administration. Finally, we tested whether unilateral photopharmacological stimulation of mGlu4 with optogluram, a photoswitchable mGlu4 PAM, in the projection site of NAc SPNs, the ventral pallidum (VP), would be sufficient to rescue social behavior in *Fmr1*$^{-/-}$ mice. In order to delineate the contribution of mGlu4 receptors expressed by NAc SPNs, we investigated whether decreasing the expression of *Grm4* in the NAc would be sufficient to prevent the restoration of social deficits by systemic mGlu4 facilitation in *Fmr1*$^{-/y}$ mice. Our results are consistent with our working hypothesis of biased D1/D2-SPN balance in ASD-like symptoms in FXS and emphasize the contribution of NAc mGlu4 receptors in alleviating such deficits.

2. Materials and methods

2.1. Ethics

This study was approved by the Comité d'Éthique en Expérimentation Animale Val de Loire (C2EA-19; APAFIS#57856–2025111817283407 and APAFIS#27791–2020102017528289). All experimental procedures were conducted in accordance with the European Communities Council Directive 2010/63/EU. Animal studies are reported in compliance with the ARRIVE guidelines [57].

2.2. Animals, housing conditions and breeding procedures

Equivalent numbers of male and female *Fmr1*$^{+/+}$ and *Fmr1*$^{-/-}$ mice (KO2, generously provided by R. Willemsen, Erasmus University Medical Center, Rotterdam, Netherlands) were bred in-house on a C57BL/6 J background. *Fmr1*$^{+/+}$ and *Fmr1*$^{-/-}$ pups were bred from homozygous parents, which were bred from heterozygous animals, to prevent genetic drift. Male and female pups in the same cage were of the same genotype: this breeding scheme and housing conditions likely exacerbated behavioral deficits in *Fmr1*$^{-/-}$ mice by maintaining them together during early post-natal development [58]. We defined sample size (G*Power 3.1) to ensure sufficient statistical power using ANOVA or Kruskal-Wallis analysis of variance to detect significant effects on our parameters (effect size f=1.80, α=0.05, σ=5, n = 8, power=0.96). Mice were weaned at 3 weeks of age. Then, cages containing either *Fmr1*$^{+/+}$ or *Fmr1*$^{-/-}$ mice (same age and sex, 2–3 mice per cage) were organized from as many different litters as possible (to limit litter effects) by the staff of the animal facility (blind to experiments) and assigned randomly to a treatment condition (same treatment in the whole cage, 4–6 cages per experimental condition). We ensured that sex ratio was equivalent between groups, and that mice from different litters met during the direct social interaction test. Except otherwise stated, animals were group-housed and maintained on a 12 hr light/dark cycle (lights on at 7:00 AM) at controlled temperature (21 ± 1°C); food and water were available *ad libitum*. Experiments were analyzed blind to genotypes and experimental conditions. All experimental procedures were conducted in accordance with the European Communities Council Directive 2010/63/EU and approved by the Comité d'Éthique en Expérimentation animale Val de Loire (C2EA-19).

2.3. Drugs for in vivo experiments

The D1/D5 dopamine receptor agonist SKF-81297 (hydrobromide), the D2/D3 dopamine receptor agonist quinpirole (hydrochloride), the non-selective dopamine receptor antagonist haloperidol (hydrochloride), the D1/D5 dopamine receptor antagonist SCH-23390 (hydrochloride), the D2/D3 dopamine receptor antagonist sulpiride, the mGlu4 PAM VU0155041 (sodium) and the A2a adenosine receptor antagonist

istradefylline were purchased from Tocris Bioscience (Bristol, UK). Morphine (hydrochloride) was obtained from Francopia (Antony, France). The mGlu4 PAM ADX88178 was purchased from abcr (Karlsruhe, Germany; ref #AB494741). The mGlu4 orthosteric agonist LSP4–2022 was synthesized in the laboratory of F.A. following previously described procedure [59]. The mGlu4 photoswitchable PAM optogluram was synthesized in the laboratory of A.L. following a previously described procedure [60]. Compounds were dissolved in sterile isotonic saline solution (NaCl 0.9%) except for istradefylline and ADX88178, suspended in 1% carboxymethyl cellulose (CMC, in NaCl 0.9%). Intraperitoneal (i.p.) or subcutaneous (s.c.) volume of injection was 10 ml/kg. Doses refer to salt weight.

2.4. RNAscope in situ hybridization

2.4.1. Sacrifice

Fmr1$^{+/+}$ and *Fmr1*$^{-/-}$ mice were tested for direct interaction for 10 min and were euthanized by cervical dislocation 45 min after the beginning of the test to capture *Fos* mRNA expression induced by the social task.

2.4.2. Brain processing and RNAscope in-situ hybridization assay

Immediately after euthanasia, fresh brain tissue was gently frozen in cryomolds with OCT on dry ice and stored at −80ºC until sectioning and running RNAscope assay (RNAscope® Multiplex Fluorescent Reagent kit v2, 323100; ACDbio, Minneapolis, USA).

Brains were sectioned using a cryostat (Leica CM1860; Leica Biosystems, Deer Park, IL, USA). Coronal 16-µm NAc slices were collected on Superfrost Plus slides (Thermo Fisher Scientific, Waltham, MA, USA) and stored at −80ºC until performing the RNAscope ISH for *Fos*, *Pdyn* and *Penk* mRNAs. We ran the RNAscope assay according to the user manual for fresh-frozen tissue. On the first day, slices were post-fixed in 4% paraformaldehyde for 15 min at 4ºC and then were dehydrated in successive ethanol baths of increasing concentration (50, 70 and 100% ethanol). Drops of RNAscope hydrogen peroxide were put on dehydrated sectionsfor 10 min at room temperature. Hydrophobic barriers were then created around sections. Sections were incubated with the RNAscope Protease IV for 30 min at 40ºC and then with a mix of probes targeting *Fos* (RNAscope® Probe – Mm-Fos-C1, 316921-C1; ACDbio, Minneapolis, USA), *Pdyn* (RNAscope® Probe – Mm-Pdyn-C2, 318771-C2; ACDbio, Minneapolis, USA), and *Penk* (RNAscope® Probe – Mm-Penk-C3, 318761-C3; ACDbio, Minneapolis, USA) mRNAs for 2 h at 40ºC. Slides were stored in 5X Saline Sodium Citrate buffer overnight at room temperature. On the second day, the signal probes were amplified by using the AMP1, 2 and 3 solutions respectively and were developed by using the HRP-C1, C2, and C3 and the fluorophore solutions for labelling the C1 probe in green (Opal 520 reagent pack, FP1487001KT; Akoya Biosciences, San Francisco, CA, USA), the C2 probe in orange (Opal 570 reagent pack, FP1488001KT; Akoya Biosciences, San Francisco, CA, USA) and the C3 probe in far red (Opal 690 reagent pack, FP1497001KT; Akoya Biosciences, San Francisco, CA, USA). The slides were washed with 1X wash buffer after each step described above. Finally, nuclei were labelled using DAPI solution, slides were mounted with ProLong^{TM} Gold antifade mountant (Thermo Fisher Scientific, Waltham, MA, USA) and stored in the dark at 2–8ºC.

2.4.3. Image acquisition

Sections of NAc Core, NAc Shell, lateral and medial DS were imaged on Zeiss Imager Z.2 microscope (Zeiss, Oberkochen, Germany). For each region, four to twenty-four images (900 µm x 700 µm, 40X magnification) from one to three serial sections (left and right hemispheres, NAc AP: +1.54 mm to +1.34 mm; DS AP: +1.34 mm to +0.98 mm) were selected for each mouse. Single-labelled *Pdyn*+ or *Penk*+ cells and double-labelled *Fos*$^{+}$-*Pdyn*$^{+}$ and *Fos*$^{+}$-*Penk*$^{+}$ cells were manually counted by two different experimenters (ImageJ v2.14.0). For each individual animal, a percentage of activated cells (mean number of double-labeled cells over mean number of single-labeled ones) was calculated for each type of SPN across images and sections; a ratio (D1-SPN/D2-SPN) was derived from these percentages.

2.5. Real-time quantitative PCR analysis

Brains were removed and placed into a brain matrix (ASI Instruments, Warren, MI, USA). PFC, DS, NAc, central amygdala (CeA) and ventral tegmental area/substantia nigra pars compacta (VTA/SNc) were punched out from 1mm-thick slices (see Figure S4A). We evaluated the expression of transcripts coding for metabotropic glutamate receptors present in cerebral tissue: mGlu1, 2, 3, 4, 5, 7 and 8 (*Grm1, 2, 3, 4, 5, 7 and 8*), marker genes of D1- and D2-SPNs (*Drd1, Drd2, Penk, Pdyn, Adora2a, Arpp21, Hpca, Nr4a1, Oprm1*) as well as genes coding for the neuropeptide oxytocin and its receptor (*Oxt, Oxtr*). Tissues were immediately frozen on dry ice and kept at −80°C until use. For each structure of interest, genotype and condition, samples were prepared and processed individually (n = 11 mice per genotype). RNA was extracted and purified using the Direct-zol RNA MiniPrep kit (Zymo Research, Irvine, CA, USA). cDNA was synthesized using the ProtoScript II Reverse Transcriptase kit (New England BioLabs, Évry-Courcouronnes, France). qRT-PCR was performed in quadruplets on a CFX384 Touch Real-Time PCR Detection System (Biorad, Marnes-la-Coquette, France) using iQ-SYBR Green Supermix (Bio-Rad, Marnes-la-Coquette, France) kit with 0.25 µl cDNA in a 12 µl final volume in Hard-Shell Thin-Wall 384-Well Skirted PCR Plates (Biorad, Marnes-la-Coquette, France). Gene-specific primers were designed using Primer3 software to obtain a 100- to 150-bp product and purchased from Sigma-Aldrich (Saint Quentin, France); sequences are displayed in Table S1. Relative expression ratios were normalized to the expression level of β-actin and the $2^{-\Delta\Delta Ct}$ method was applied to evaluate differential expression level.

2.6. In cellulo pharmacology

2.6.1. Cell culture

Fmr1$^{-/-}$ and *Fmr1*$^{+/+}$ HEK293 cells (CL0044661816A) were obtained from Edigene (Beijing, China). Cells were cultured in Dulbecco's modified Eagle medium (DMEM) complemented with 10% fetal bovine serum (Thermo Fisher Scientific, Waltham, MA, USA). Cells were maintained at 37°C in a humidified atmosphere with 5% CO_2. Cells were transiently transfected with human A2a, mGlu4 or mGlu5 using lipofectamine 2000 (Thermo Fisher Scientific, Waltham, MA, USA) following the manufacturer's recommendations. All receptors contained a N-terminal SNAP-tag to determine their cell-surface expression. Following transfection, cells were seeded overnight at 100,000 per well into black, clear-bottom 96-well culture plates (Greiner Bio-One, Courtaboeuf, France). Cell-surface expression of the receptors and pharmacological experiments were performed 24 h after transfection.

2.6.2. Cell-based pharmacological assays

The activation of A2a and mGlu4 receptors was evaluated by measuring cAMP accumulation, reflecting their coupling to the G_s and $G_{i/o}$ pathways, respectively. cAMP levels were quantified using assay kits from Cisbio Bioassays (Codolet, France), following the manufacturer's instructions. mGlu5 receptor activation, which signals through the G_q pathway, was assessed by monitoring intracellular Ca^{2+} release using the fluorescent probe Fluo4-AM (Thermo Fisher Scientific, Waltham, MA, USA), as previously described [61]. Cells were exposed to increasing concentrations of reference agonists (Tocris Biosciences, Bristol, UK): NECA for A2a receptors, L-AP4 for mGlu4 receptors (in the presence of 300 nM forskolin), and quisqualate for mGlu5 receptors.

2.6.3. Cell-surface expression

Cell surface receptor expression was assessed using SNAP-tagged receptors labeled with Lumi4-Tb. Twenty-four hours after transfection, cells were incubated with SNAP-Lumi4-Tb, washed with Tag-Lite buffer,

and the fluorescence signal was subsequently measured (Cisbio Bioassays, Codolet, France).

2.7. Behavioral experiments

Equivalent numbers of naive male and female animals were used in each group except for the *Grm4*-targeting shRNA experiment in which only male mice were used. All animals were aged 8–12 weeks at the beginning of experiments. Acute pharmacological treatment (Figs. 1, 6 and S7) and RNAscope experiments (Fig. 2) were performed in independent cohorts of naive mice. For each chronic treatment experiment, behavioral tests were performed successively in a dedicated cohort of naive mice (Figs. 3–5), except for the istradefylline experiment, for which two cohorts were used (see timeline of experiments in Figure S8). Behavioral testing order was chosen to minimize the incidence of anxiety generated by each test on later assays. Experiments were conducted and analyzed blind to genotype and experimental condition.

2.7.1. Locomotor activity under pharmacological challenge or chronic treatment

Locomotor activity was assessed in clear Plexiglas boxes (21 × 11 × 17 cm) placed over a white Plexiglas infrared-lit platform. Light intensity of the room was set at 15 lx. The trajectories of the mice were analyzed and recorded via an automated tracking system equipped with an infrared-sensitive camera (Videotrack; View Point, Lyon, France). To focus on forward activity, only movements whose speed was over 6 cm/s were considered for the measurement of locomotor activity.

When monitoring the effects of dopamine receptor agonists, mice were placed in the activity boxes for a habituation period of 60 min before SKF-81297 administration (to obtain stable low activity) and 15 min before quinpirole injection (to avoid a floor effect when measuring locomotor inhibition). Mice were then injected with either vehicle (NaCl 0.9%), SKF-81297 (0.5, 1 or 2 mg/kg, s.c.) or quinpirole (0.05 or 0.1 mg/kg, s.c.), and locomotor activity was monitored for further 80 min (SKF-81297) or 60 min (quinpirole). For testing VU0155041 effects, locomotor activity was measured over 60 min, starting 30 min after daily administration (D9) of the mGlu4 PAM treatment (5 mg/kg, i.p. versus vehicle – NaCl 0.9%). The total traveled distance was calculated for the entire time course; for quinpirole experiment, a second calculation (first 30 min) was performed to avoid counting the potential biphasic effects of low-to-moderate used doses [62].

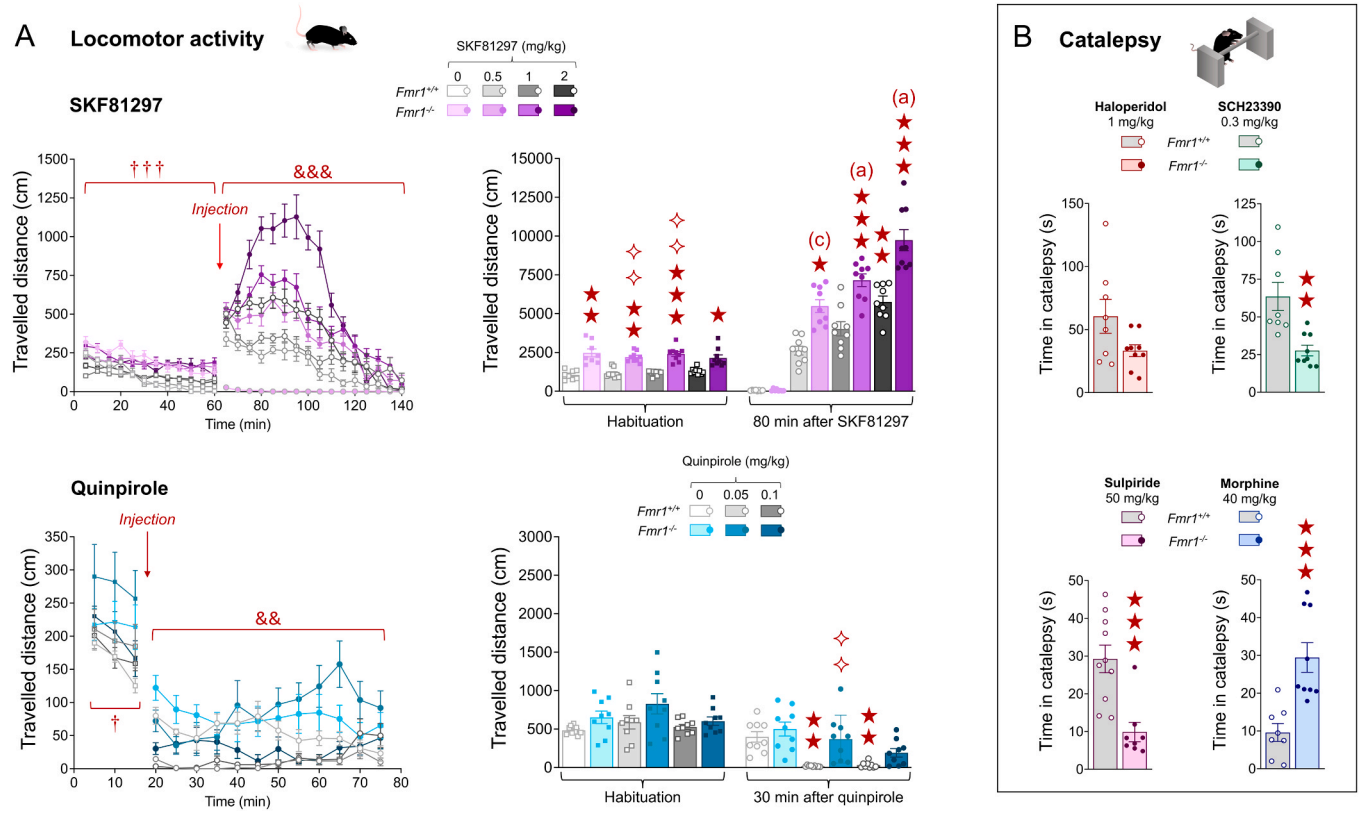


Fig. 1. Effects of dopaminergic drugs on locomotor activity and catalepsy in *Fmr1*$^{-/-}$ mice. (A) Adult *Fmr1*$^{+/+}$ and *Fmr1*$^{-/-}$ mice received the dopamine D1/D5 receptor agonist SKF-81297 (0, 0.5, 1 and 2 mg/kg, s.c.; n = 8–9 mice per group) or the D2/D3 receptor agonist quinpirole (0, 0.05 and 0.1 mg/kg, s.c.; n = 9 mice per group) after a 60 or 15-min habituation period, respectively. *Fmr1*$^{-/-}$ mice were more active than *Fmr1*$^{+/+}$ mice during habituation (SKF-81297, time course: *G:* $F_{1,46}$=*88.1, p < 0.001*; travelled distance in 80 min: $H_{7,70}$=*52.5, p < 0.001*; quinpirole, time course: *G:* $F_{1,48}$=*6.5, p < 0.05;* travelled distance in 30 min: $H_{5,54}$=*8.4, NS*). SKF-81297 produced higher locomotor stimulation in *Fmr1*$^{-/-}$ compared to *Fmr1*$^{+/+}$ mice (time course: *G x T x D:* $F_{30,690}$=*3.1, p < 0.001;* travelled distance in 80 min: $H_{7,70}$=*61.7, p < 0.001*). Conversely, quinpirole exhibited a reduced efficacy in decreasing locomotion in *Fmr1*$^{-/-}$ mice (time course: *G x T x D:* $F_{22,528}$=*2.0, p < 0.01*; travelled distance in 30 min: $H_{5,54}$=*35.1, p < 0.001*). (B) Independent groups of adult *Fmr1*$^{+/+}$ and *Fmr1*$^{-/-}$ mice received the dopaminergic antagonist haloperidol (D1/D2 dopamine receptors, 1 mg/kg), the D1/D5 receptor antagonist SCH-23390 (0.3 mg/kg), the D2/D3 receptor antagonist sulpiride (50 mg/kg) 30 min prior testing or the opioid receptor agonist morphine (40 mg/kg) 60 min prior testing. Haloperidol induced a similar cataleptic response in *Fmr1*$^{+/+}$ and *Fmr1*$^{-/-}$ mice; SCH-23390 (*U=4.0, p = 0.001*) and sulpiride (*U=4.0, p < 0.001*) produced shorter cataleptic responses in *Fmr1*$^{-/-}$ mice compared to *Fmr1*$^{+/+}$ mice. Conversely, *Fmr1*$^{-/-}$ mice treated with morphine spent longer time in catalepsy than *Fmr1*$^{+/+}$ mice (*U=2.0, p < 0.001*). Results are shown as scatter plots and mean ± SEM. Daggers: genotype effect; ampersands: genotype x time x dose interaction; solid stars: comparison with the vehicle-treated *Fmr1*$^{+/+}$ group in locomotor activity experiments (either during habituation or after compound administration), and with the *Fmr1*$^{+/+}$ group in catalepsy assays; diamonds: comparison with the *Fmr1*$^{+/+}$ group treated by the same dose of treatment. One symbol: $p < 0.05$; two symbols: $p < 0.01$; three symbols: $p < 0.001$. Letters: comparison with vehicle-treated *Fmr1*$^{-/-}$ group; (c): $p < 0.05$, (b): $p < 0.01$, (a): $p < 0.001$. Abbreviations: D: dose; G: genotype; NS: not significant; T: time.

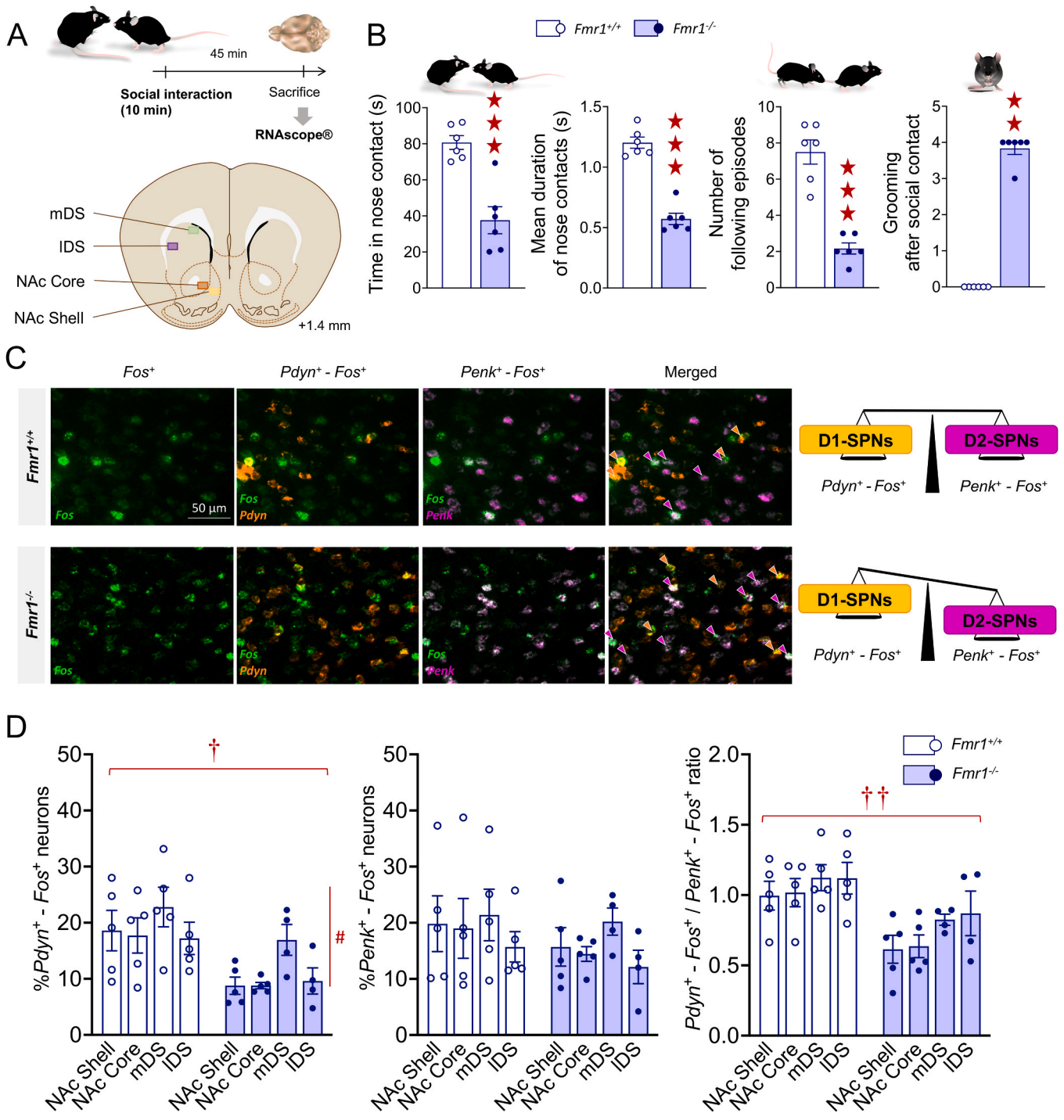


Fig. 2. Assessment of *Fos*-positive of D1- and D2-SPNs following direct social interaction in *Fmr1*$^{-/-}$ mice using RNAscope® hybridization. (A) Experimental design. Adult *Fmr1*$^{+/+}$ and *Fmr1*$^{-/-}$ mice (n = 6 per group) performed a direct social interaction test (10 min). Mice were euthanized 45 min after the beginning of the interaction test, brain were removed and frozen at −80°C for RNAscope® experiments. (B) In the direct social interaction test, *Fmr1*$^{-/-}$ mice displayed a severe deficit in social behavior, as evidenced by decreased time spent in (*G: $F_{1,10}$=26.0, $p < 0.001$*) and mean duration of (*G: $F_{1,10}$=89.0, $p < 0.001$*) nose contacts, number of following episodes (*G: $F_{1,10}$=52.2, $p < 0.001$*), associated with an increase in the number of grooming episodes after social contact (*U=0.0, $p < 0.01$*). More behavioral parameters are available in Fig. S3A. (C) Representative microphotographs of the NAc Core showing *Fos*-labelled nuclei (green probe), *Pdyn*-labelled neurons (D1-SPNs, orange probe) and *Penk*-labelled neurons (D2-SPNs, red probe) in *Fmr1*$^{+/+}$ (upper panel) and *Fmr1*$^{-/-}$ (lower panel) mice using the RNAscope® hybridization technique. Magnification: 40x, Scale bar: 50 µm. (D) We detected a decreased proportion of *Pdyn*$^{+}$ (D1-SPNs)-*Fos*$^{+}$ neurons in the whole striatum of *Fmr1*$^{-/-}$ mice (*G: $F_{1,10}$=9.3, $p < 0.05$*), while the percentage of *Penk*$^{+}$ (D2-SPNs)-*Fos*$^{+}$ neurons was unaffected. As a consequence of this, the ratio of *Pdyn*$^{+}$-*Fos*$^{+}$ / *Penk*$^{+}$-*Fos*$^{+}$ neurons was globally decreased in the striatum of *Fmr1*$^{-/-}$ mice (*G: $F_{1,10}$=10.3, $p < 0.01$*). There was no difference in the total number of *Pdyn*$^{+}$ and *Penk*$^{+}$ neurons between *Fmr1*$^{+/+}$ and *Fmr1*$^{-/-}$ mice (Fig. S3B). Behavioral and hybridization data are shown as scatter plots and mean ± SEM. Solid stars: comparison with the *Fmr1*$^{+/+}$ group; daggers: genotype effect; hashtag: region effect. One symbol: $p < 0.05$; two symbols: $p < 0.01$; three symbols: $p < 0.001$. Abbreviations: G: genotype effect; lDS: dorsal striatum, lateral part, mDS: DS, medial part; NAc Core: core of the nucleus accumbens; NAc Shell: shell of the nucleus accumbens.

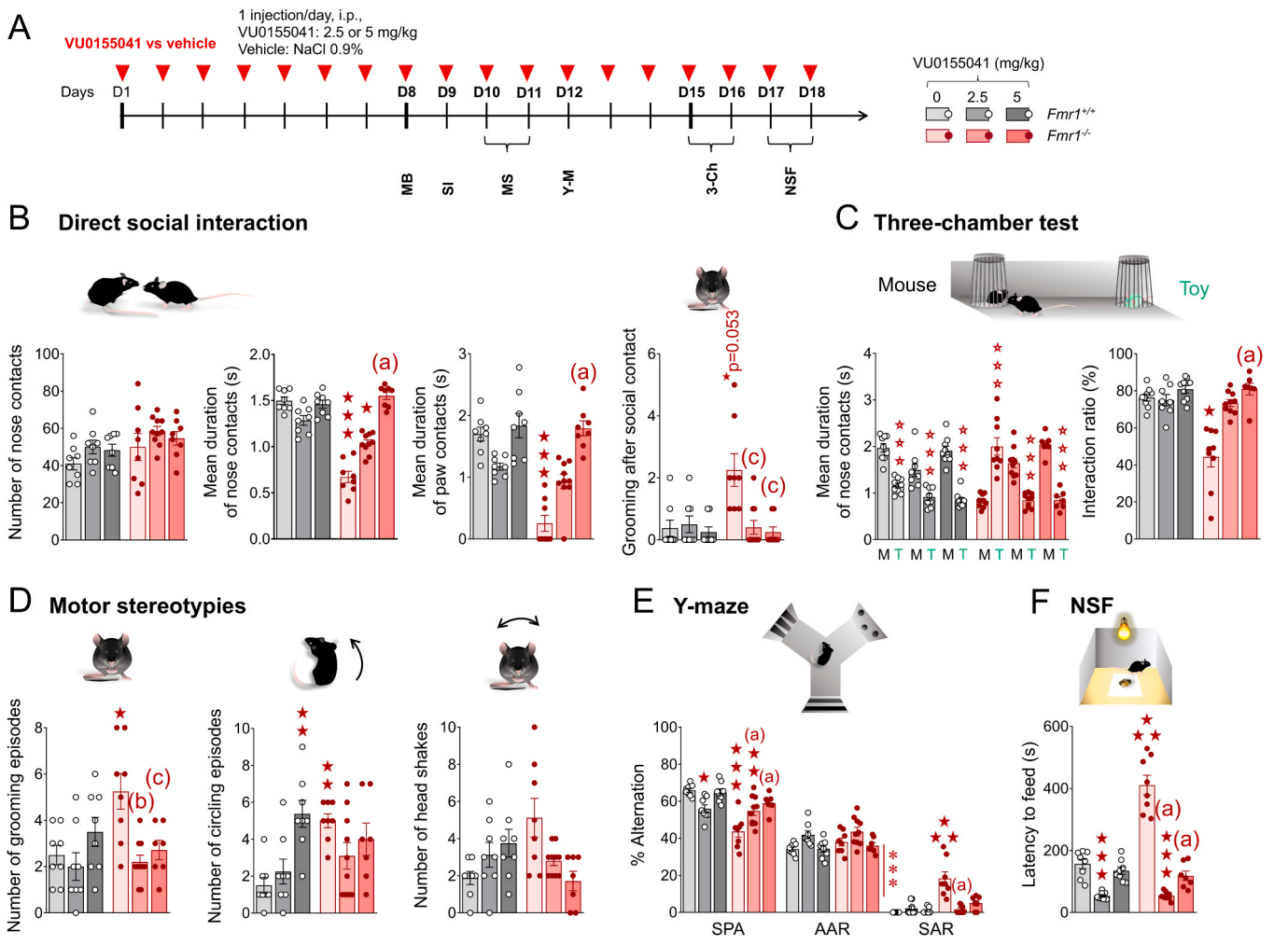


Fig. 3. Effects of chronic facilitation of mGlu4 activity on social behavior, motor stereotypies, perseverative behavior and anxiety-like levels in *Fmr1*$^{-/-}$ mice. (A) A first cohort of *Fmr1*$^{+/+}$ and *Fmr1*$^{-/-}$ mice (n = 7–10 per group) was injected once daily with either VU0155041 (2.5 or 5 mg/kg, i.p.) or vehicle (NaCl 0.9%) for 18 days. Behavioral testing started on D8. (B) In the direct social interaction test, chronic VU0155041 administration dose-dependently normalized nose ($H_{5,50}$=*41.2, p < 0.001*) and paw ($H_{5,50}$=*36.4, p < 0.001*) contact duration as well as grooming after social contact ($H_{5,50}$=*18.6, p < 0.01*) in *Fmr1*$^{-/-}$ mice. (C) In the three-chamber test, VU0155041 restored the preference for spending longer time (*G x Tr x S:* $F_{2,46}$=*41.7, p < 0.001*) with the mouse versus the toy, and preference ratio ($H_{5,52}$=*28.1, p < 0.001*) since the 2.5 mg/kg dose. (D) Chronic VU0155041 treatment normalized the number of stereotypic grooming (*G x Tr:* $F_{2,43}$=*3.5, p < 0.05*) and circling episodes (*G x Tr:* $F_{2,43}$=*6.5, p < 0.01*) in *Fmr1*$^{-/-}$ mice. (E) In the Y-maze, VU0155041 restored spontaneous alternation (SPA; *G x Tr:* $F_{2,43}$=*12.5, p < 0.001*) and suppressed perseverative same arm returns (SAR; $H_{5,49}$=*29.5, p < 0.001*). (F) In the novelty-suppressed feeding test, both doses of VU0155041 fully normalized the latency to feed (*G x Tr:* $F_{2,43}$=*44.5, p < 0.001*). Results are shown as scatter plots and mean ± SEM. Solid stars: comparison with the vehicle-treated *Fmr1*$^{+/+}$ group; open stars: genotype x treatment x stimulus interaction, mouse versus toy comparison; asterisks: treatment effect. One symbol: p < 0.05; two symbols: p < 0.01; three symbols: p < 0.001. Letters: comparison with vehicle-treated *Fmr1*$^{-/-}$ group; (c): p < 0.05, (b): p < 0.01, (a): p < 0.001. More behavioral parameters are available in Fig. S6. Abbreviations: 3-Ch: three-chamber test; AAR: alternate arm returns; G: genotype effect; M: mouse; MB: marble burying test; MS: motor stereotypies; NSF: novelty-suppressed feeding test; S: stimulus effect; SAR: same arm returns; SI: social interaction test; SPA: spontaneous alternation; T: toy; Tr: treatment effect; Y-M: Y-maze test.

2.7.2. Catalepsy

This behavior was assessed as an indicator of striatal function [63,64]. Each animal was injected with the test compound or saline (i.p. or s.c.), and the catalepsy procedure was measured using the bar test, 30 min after haloperidol (1 mg/kg), SCH-23390 (0.3 mg/kg) or sulpiride (50 mg/kg) injection, and 60 min after morphine injection (40 mg/kg). The forelimbs of each experimental mouse were placed on a cylindrical plastic bar (straw, diameter: 0.4 cm) clipped in Lego bricks 3.5 cm above the table. The time during which both forelimbs remained on the bar was recorded. The test was repeated four times (inter-trial interval: 30 s).

2.7.3. Social abilities

Direct social interaction test. The experimental protocol was adapted from [65,66]. On testing day, a pair of unfamiliar mice (not cage mates, age-, sex-, genotype- and treatment-matched) was introduced in one of 4 square arenas (50 ×50 cm, separated by 35 cm-high opaque grey Plexiglas walls) over a white infrared floor (View Point, Lyon, France) for 10 min (15 lx). Each arena received a black plastic floor (transparent to infrared) to minimize anxiety levels. The total amount of time spent in nose contact (nose-to-nose, nose-to-flank and nose-to-anogenital region), the number of these contacts, the time spent in paw contact and the number of these contacts, grooming episodes (self-grooming), notably ones occurring immediately (<5 s) after a social contact, as well as the number of following episodes were scored *a posteriori* on video recordings (infrared light-sensitive video camera) using an ethological keyboard (Labwatcher®, View Point, Lyon, France) by trained experimenters, and individually for each animal. The mean duration of nose and paw contacts was calculated as the total time spent in these events divided by the number of events.

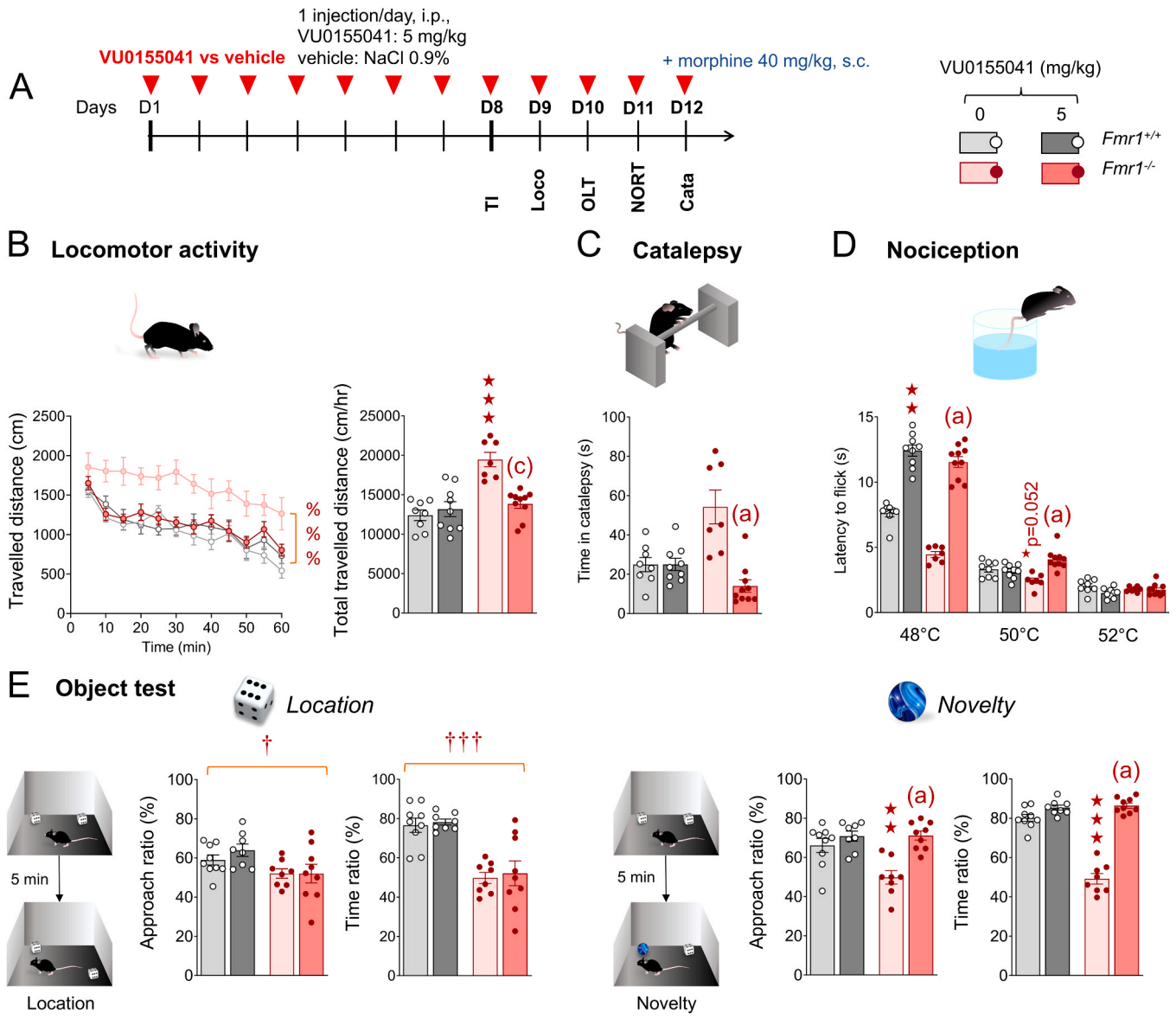
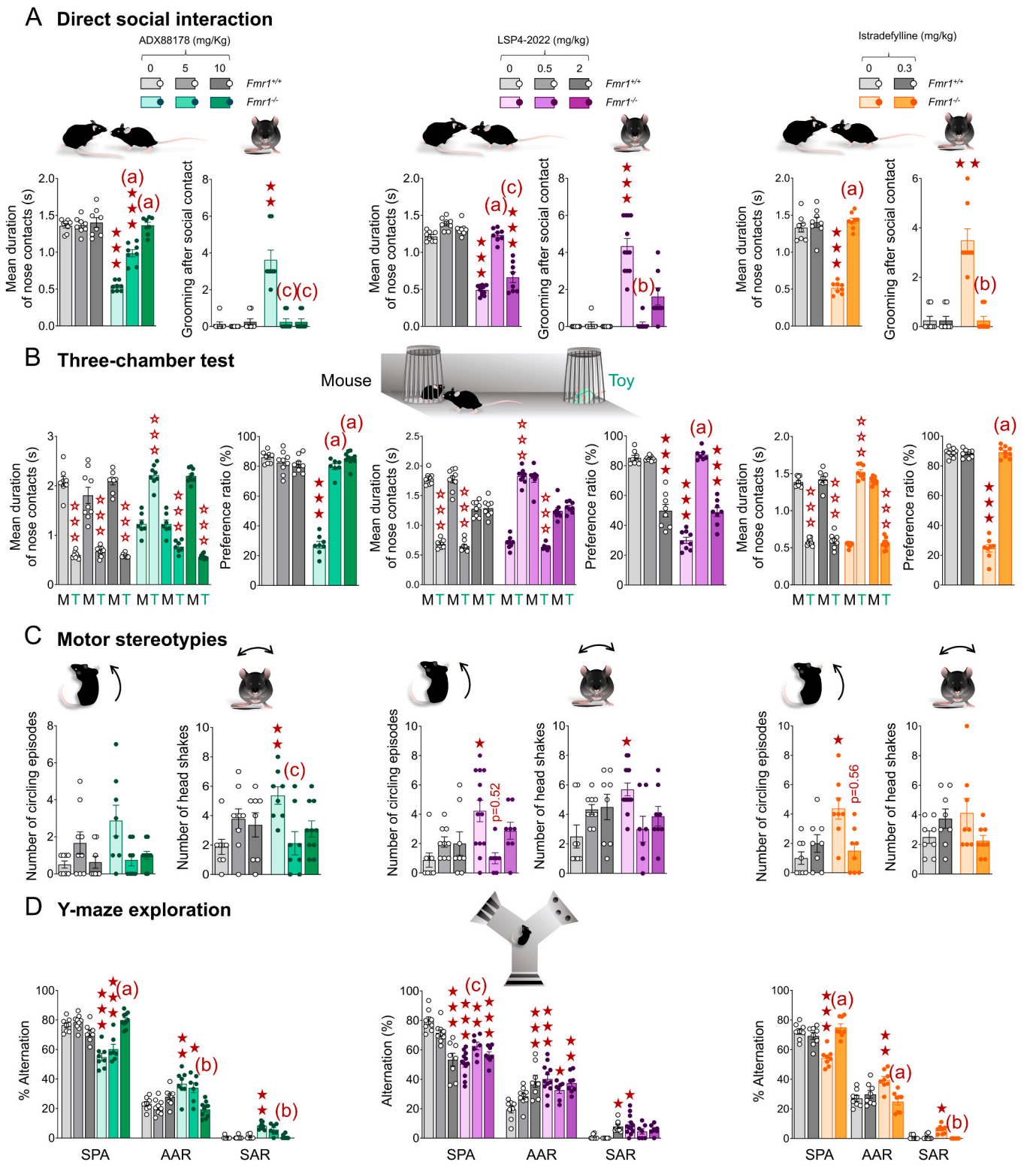


Fig. 4. Effects of chronic facilitation of mGlu4 activity on locomotor activity, catalepsy, nociception and cognition in *Fmr1*$^{-/-}$ mice. (A) A cohort of *Fmr1*$^{+/+}$ and *Fmr1*$^{-/-}$ mice (n = 8–9 per group) was injected once daily with either VU0155041 (5 mg/kg, i.p.) or vehicle (NaCl 0.9%) for 12 days. (B) In the locomotor activity recording test, *Fmr1*$^{-/-}$ mice displayed hyperactivity that was suppressed by VU0155041 treatment (time course: *G x Tr:* $F_{11,330}$*=16.6, p < 0.001,* travelled distance in 60 min: $H_{3,34}$*=16.8, p < 0.001*). (C) Following morphine administration (40 mg/kg, s.c.), *Fmr1*$^{-/-}$ mice spent longer time in catalepsy, normalized by VU0155041 ($H_{3,34}$*=18.0, p < 0.001*). (D) In the tail immersion test, VU0155041 increased nociceptive thresholds in both mouse lines at 48°C ($H_{3,34}$*=27.3, p < 0.001*). At 50°C, VU0155041 increased the latency to flick in *Fmr1*$^{-/-}$ mice (*G x Tr:* $F_{1,30}$*=16.7, p < 0.001*). (E) In the object location test, *Fmr1*$^{-/-}$ mice displayed reduced approach (*G:* $F_{1,30}$*=7.5, p < 0.05*) and time (*G:* $F_{1,30}$*=40.6, p < 0.001*) ratios, without VU0155041 effects. In the novel object recognition test, the deficit detected in *Fmr1*$^{-/-}$ mice was rescued by VU0155041 administration (approach: *G x Tr:* $F_{1,30}$*=7.5, p < 0.05;* time*: G x Tr:* $F_{1,30}$*=78.2, p < 0.001*). Results are shown as scatter plots and mean ± SEM. Percents: genotype x treatment interaction; solid stars: comparison with the vehicle-treated *Fmr1*$^{+/+}$ group; daggers: genotype effect. One symbol: $p < 0.05$; two symbols: $p < 0.01$; three symbols: $p < 0.001$. Letters: comparison with vehicle-treated *Fmr1*$^{-/-}$ group; (c): $p < 0.05$, (a): $p < 0.001$. Abbreviations: Cata: catalepsy; G: genotype effect; Loco: locomotor activity; OLT: object location test; NORT: novel object recognition test; Tr: treatment effect; TI: tail immersion.

Three-chamber social preference test. The experimental protocol was adapted from [65,67]. The test apparatus consisted of a grey external Plexiglas box with transparent partitions dividing the box into three equal chambers (40 ×20 x 22.5 cm). Two sliding doors (8 ×5 cm) allowed transitions between chambers. Cylindrical wire cages (18 ×9 cm, 0.5 cm diameter-rods spaced 1 cm apart) were used to contain the mouse interactors and object (soft toy mouse) placed in the two outward chambers of the 3-chamber social preference test. The test was performed under low-light conditions (15 lx) to reduce anxiety. Stimulus *Fmr1*$^{+/+}$ mice were habituated to wire cages for 2 days before the test (20 min/day). On testing day, the experimental mouse was introduced to the middle chamber and allowed to explore the whole apparatus for a 10-min habituation phase (wire cages empty). For the social preference phase, the experimental mouse was confined back in the middle-chamber while the experimenter introduced an unfamiliar *Fmr1*$^{+/+}$ age and sex-matched mouse (8–14-week-old, grouped housed) into a wire cage in one of the side-chambers and a soft toy mouse (8 ×10 cm) in the second wire cage. Then, the experimental mouse was allowed to explore the apparatus for 10 min. The sliding doors were reopened allowing an additional 10-min exploration. The time spent in each chamber and in nose contact with each wire cage, the number of these contacts and the number of entries in each chamber were scored *a posteriori* on video recordings using an ethological keyboard (Labwatcher®, View Point, Lyon, France) by trained experimenters. The



(caption on next page)

Fig. 5. Compared effects of chronic mGlu4 facilitation or orthosteric activation, and adenosine A2a receptor blockade on core ASD-like symptoms in *Fmr1*$^{-/-}$ mice. (A) In the direct social interaction test, ADX88178 (n = 8–10 per group) dose-dependently restored the mean duration of nose contacts (*G x Tr:* $F_{2,42}$*=40.5,* $p < 0.001$) and suppressed grooming after social contact since the dose of 5 mg/kg ($H_{5,48}$*=30.4,* $p < 0.001$). LSP4-2022 (n = 8–13 per group) demonstrated beneficial effects on social parameters at 0.5 but not 2 mg/kg (nose contact duration: *G x Tr:* $F_{2,46}$*=36.3,* $p < 0.001$, grooming after social contact: $H_{5,52}$*=43.6,* $p < 0.001$). Istradefylline (n = 8–9 per group) restored social interaction (nose contact duration: *G x Tr:* $F_{1,28}$*=65.7,* $p < 0.001$, grooming after social contact: $H_{3,32}$*=21.5,* $p < 0.001$). (B) In the three-chamber test, ADX88178 rescued social preference (duration of nose contacts: *G x Tr x S:* $F_{2,44}$*=297.3,* $p < 0.001$, preference ratio: *G x Tr:* $F_{2,44}$*=150.0,* $p < 0.001$). LSP4-2022 restored social preference at 0.5 mg/kg; both *Fmr1*$^{+/+}$ and *Fmr1*$^{-/-}$ mice treated at the dose of 2 mg/kg failed to discriminate between the mouse and the toy (duration of nose contacts: *G x Tr x S:* $F_{2,47}$*=64.4,* $p < 0.001$, preference ratio: *G x Tr:* $F_{2,47}$*=42.3,* $p < 0.001$). Istradefylline normalized social preference (duration of nose contacts: *G x Tr x S:* $F_{1,30}$*=614.6,* $p < 0.001$, preference ratio: *G x Tr:* $F_{1,30}$*=442.7,* $p < 0.001$). (C) All three compounds reduced motor stereotypies in *Fmr1*$^{-/-}$ mice (ADX88178 - head shakes: *G x Tr:* $F_{2,45}$*=7.8,* $p < 0.01$; LSP4-2022 - circling episodes: $H_{5,53}$*=17.1,* $p < 0.01$; head shakes: $H_{5,53}$*=12.8,* $p < 0.05$; istradefylline - circling episodes: $H_{3,32}$*=11.9,* $p < 0.01$). (D) In the Y-maze, ADX88178 restored SPA in *Fmr1*$^{-/-}$ mice at 10 mg/kg (*G x Tr:* $F_{2,44}$*=31.4,* $p < 0.001$), by reducing AAR (*G x Tr:* $F_{2,44}$*=16.0,* $p < 0.001$) and SAR ($H_{5,50}$*=34.3,* $p < 0.001$). Low dose of LSP4-2022 partially restored SPA (*G x Tr:* $F_{2,46}$*=17.5,* $p < 0.001$) in *Fmr1*$^{-/-}$ mice but failed to restore AAR (*G x Tr:* $F_{2,46}$*=8.2,* $p < 0.001$) and SAR ($H_{5,52}$*=27.8,* $p < 0.001$). At 2 mg/kg, LSP4-2022 altered the pattern of alternation of *Fmr1*$^{+/+}$ mice. Finally, istradefylline restored SPA (*G x Tr:* $F_{1,28}$*=29.7,* $p < 0.001$) by reducing AAR (*G x Tr:* $F_{1,28}$*=14.0,* $p < 0.001$) and SAR ($H_{3,32}$*=20.8,* $p < 0.001$) in *Fmr1*$^{-/-}$ mice. Results are shown as scatter plots and mean ± SEM. Solid stars: comparison with the vehicle-treated *Fmr1*$^{+/+}$ group; open stars: genotype x treatment x stimulus interaction, mouse versus toy comparison. One symbol: $p < 0.05$; two symbols: $p < 0.01$; three symbols: $p < 0.001$. Letters: comparison with vehicle-treated *Fmr1*$^{-/-}$ group; (c): $p < 0.05$, (b): $p < 0.01$; (a): $p < 0.001$. Abbreviations: AAR: alternate arm returns; D: day; G: genotype effect; M: mouse; S: stimulus effect; SAR: same arm returns; SPA: spontaneous alternation; T: toy; Tr: treatment effect. The timeline of experiments and additional behavioral parameters are available in Fig. S8.

mean duration of nose contacts (nose to nose, nose to flank, nose to anogenital region) was calculated from these data. Preference ratio was calculated as follows: Time in nose contact with the mouse / (Time in nose contact with the mouse + Time in nose contact with the object) x 100. The relative position of stimulus mice was counterbalanced between groups.

2.7.4. Stereotyped and perseverative behaviors

Motor stereotypies. The experimental protocol was adapted from [68]. To detect spontaneous motor stereotypies in *Fmr1*$^{-/-}$ versus *Fmr1*$^{+/+}$ animals, mice were individually placed in clear standard home cages (21 × 11 × 17 cm) filled with 3-cm deep fresh sawdust for 10 min. No water was available. Light intensity was set at 30 lx. Trained experimenters scored numbers of spontaneous head shakes, rearing, burying, grooming and circling episodes and the total amount of time spent burying by direct observation.

Marble-burying. Marble burying was used as a measure of stereotyped/perseverative behavior [67,69]. Mice were introduced individually in transparent cages (21 × 11 × 17 cm) containing 20 glass marbles (diameter: 1.5 cm) evenly spaced on 4-cm deep fresh sawdust. To prevent escapes, each cage was covered with a filtering lid. Light intensity in the room was set at 40 lx. The animals were removed from the cages after 15 min, and the number of marbles buried more than half in sawdust was recorded.

Y-maze exploration. Spontaneous alternation behavior was used to assess perseverative behavior [70,71]. Each Y-maze (Imetronic, Pessac, France) consisted of three connected Plexiglas arms (15 ×15 x 17 cm) covered with distinct wall patterns (15 lx). Floors were covered with lightly sprayed fresh sawdust to limit anxiety. Each mouse was placed at the center of the maze and allowed to freely explore this environment for 5 min. The pattern of entries into each arm was quoted on video-recordings. Spontaneous alternations (SPA), i.e. successive entries into each arm forming overlapping triplet sets, alternate arm returns (AAR) and same arm returns (SAR) were scored, and the percentage of SPA, AAR and SAR was calculated as following: total / (total arm entries −2) * 100.

2.7.5. Anxiety-like behavior

Novelty-suppressed feeding. The protocol was adapted from [72]. Novelty-suppressed feeding (NSF) was measured in 24-hr food-deprived mice, isolated in a standard housing cage for 30 min before individual testing. This test was performed in the same arenas as the ones used for direct social interaction. Three pellets of ordinary lab chow were placed on a white tissue in the center of each arena, lit at 60 lx. Each mouse was placed in a corner of an arena and allowed to explore for a maximum of 15 min. Latency to feed was measured as the time necessary to bite a food pellet. Immediately after an eating event, the mouse was transferred back to home cage (free from cage-mates) and allowed to feed on lab chow for 5 min. Food consumption in the home cage was measured.

2.7.6. Nociceptive thresholds

Tail-immersion test. This test was performed as previously described [42,73]. Nociceptive thresholds were assessed by immersing the tail of the mice (5 cm from the tip) successively into water baths at 48°C, 50°C and 52°C. Mice were gently maintained in a tissue pocket during this experiment. The latency to withdraw the tail was measured at each temperature, with a cut-off of 10 s.

2.7.7. Cognitive performance

Object location and novel object recognition test. The experimental paradigm was adapted from [74]. The test was performed on two successive days. On day 1, during familiarization phase (10 min), the mice were presented with two copies of an unfamiliar object. The animals were returned to their home cage for a 5 min intertrial interval. During this interval, the experimenter displaced one of the two objects to a novel location in the arena, before the mice were allowed to freely explore the apparatus for 10 min (location phase). On day 2, during familiarization phase (10 min), the mice were presented a pair of novel unfamiliar objects. They were returned to their home cage for 5 min. During this interval, the experimenter replaced one of the two objects by a novel object. Then the mice were allowed to explore freely the arena for another 10 min (novelty phase). Stimuli objects sized 1.5–3 × 2–3 cm. The identity of the objects and their spatial location were balanced between subjects. The number of visits and the time spent exploring each object were scored *a posteriori* on video recordings. A percentage of discrimination was calculated for number of visits and time exploring the objects as following: exploration of displaced or novel object / total exploration * 100.

2.8. Photopharmacology experiments

2.8.1. Surgery

Group-housed 2-month-old male and female mice were used in this experiment. Surgeries were performed under chemical anesthesia (ketamine at 50 mg/kg and xylazine at 7.5 mg/kg). We used an optofluidic device (OsFC_240/250–0.63_5mm_FLT_100/170_0.05; Doric Lenses, Quebec, QC, Canada) to both deliver the optogluram, a light-sensitive mGlu4 PAM, and control it by light. The injection cannula (inner diameter: 100 µm; outer diameter 170 µm) coupled to an optic fiber (inner diameter: 240 µm; outer diameter 250 µm, numerical aperture = 0.63) was implanted unilaterally in the ventral pallidum at the following stereotaxic coordinates: AP: +0.55 mm; ML: +/-1.3 mm (counterbalanced right and left hemispheres); DV: −4.9 mm. It was fixed on the

skull by using dental acrylic cement. After surgery, each mouse was placed on a heat mat for a two-hour recovery before being returned to its home cage, and i.p. injections of Metacam® (2 mg/kg) were given for analgesia until the end of convalescence. Mice with incorrect cannula placement were excluded from this experiment (n = 2, one *Fmr1*$^{-/-}$ and one *Fmr1*$^{+/+}$).

2.8.2. Photopharmacology

We used photopharmacology to modulate mGlu4 activity in the VP combining two wavelengths coupled to a rotating optical fiber. Each channel was controlled via the LED driver software (Doric Lenses, Quebec, QC, Canada). After 3 weeks of recovery, mice were habituated to the optic fiber connection one week before the tests.

Optogluram (30 μM, 0.5 μl), a light-sensitive mGlu4 PAM, was injected unilaterally in the VP, through the cannula coupled with optic fiber 20 min before starting behavioral testing. We controlled optogluram activity by switching it from active (resting) to inactive state (by delivering violet light, 380 nm wavelength, 50 ms light pulses at 10 Hz) state, then back to active state (green light, 500 nm wavelength, 50 ms light pulses at 10 Hz). Social behavior was assessed in *Fmr1*$^{+/+}$ and *Fmr1*$^{-/-}$ mice using the direct social interaction test. Each fiber-implanted mouse was introduced with an unfamiliar mouse (sex, age, genotype-matched, not implanted) in a square arena (50 ×50 cm, separated by 35 cm-high opaque grey Plexiglas walls) over a black infrared floor (View Point, Lyon, France) for 9 min (15 lx). Behavioral sessions were divided into three phases: the 3-min baseline, when the light was OFF (and optogluram active), the following 3-min, when the violet light was ON (and optogluram inactive) and the last 3-min when the light was switched to green (and optogluram returned to its active state). After another 3 weeks, all the mice underwent the same protocol after intra-VP injection of vehicle, to assess the effects of light *per se*. Finally, brains were collected to verify cannula implantation sites.

2.9. Grm4-targeting shRNA experiment

2.9.1. Viral vectors

Recombinant shRNA-encoding adeno-associated virus (rAAV) vectors of serotype 9 were generated by a triple transfection of HEK293T-derived cell line with the following plasmids: pAAV-CMV-eGFP-U6-shGrm4 (transgene expression), pAAV2/9 helper encoding the AAV serotype 9 capsid and pHelper (Agilent Technologies, Santa Clara, CA, USA) encoding the adenovirus helper functions. The vectors were purified by ultracentrifugation on Iodixanol (Optiprep™ density gradient medium) gradient, dialyzed against phosphate-buffered saline (PBS) and concentrated by ultrafiltration (Amicon Ultra-15 Centrifugal Filter Devices 100 K; Millipore, Molsheim, France). Their titer (genome copies/ml) was evaluated by qPCR. In the transgene expression plasmid, the shRNA sequence is expressed under the control of the mU6 promoter, while the enhanced green fluorescent protein (eGFP) is expressed under the control of the cytomegalovirus promoter to label transduced cells. The shRNA sequence targeting the Grm4 transcript (anti-Grm4 shRNA; 5′- GCTCCCGACTTGAGTGATAAC −3′) was selected using the BLOCK-iT RNAi Designer algorithm (Thermo Fisher Scientific, Waltham, MA, USA). A scrambled sequence (scramble shRNA; 5′- GCGCTTAGCTG-TAGGATTC −3′) was used as negative control. Loop sequence was 5′-AGTCGACA-3′ for both. The rAAVs of serotype 9 bearing the anti-Grm4 shRNA sequence (titer of 10^{13} genome copies/ml) were used for behavioral experiments.

2.9.2. Validation of Grm4-targeting shRNA experiment

In cellulo validation: HEK293FT cells were cultured in DMEM supplemented with 10% fetal bovine serum (Eurobio Scientific, Les Ulis, France), 1 mM L-glutamine (Eurobio Scientific, Les Ulis, France), and penicillin/streptomycin (100 U/ml, Life Technologies, Saint-Thomas, France). Cells were maintained at 37°C in a humidified atmosphere with 5% CO_2. Cells were co-transfected with mouse c-myc-tagged mGlu4 receptor (Origen, Herford, Germany) and either 0.5 or 1 μg of eGFP-tagged shRNA-expressing plasmid using Metafectene Pro (Biontex, Munich, Germany). Forty hours after transfection, cells were harvested for qRT-PCR analyses. qRT-PCR experiments were performed as described above.

Ex vivo validation in wild-type mice: Mice were deeply anesthetized at the age of 8 weeks and placed on a stereotaxic frame, as described above. The stereotaxic injection of rAAVs (0.4×10^9 genome copies diluted in 0.01 M PBS) expressing either anti-*Grm4* or scramble shRNA was performed in the NAc (coordinates from bregma: AP +1.7 mm; ML ±0.9 mm; DV −4.6 mm) using a Hamilton syringe (Neuros 1 μl; Hamilton Company, Reno, NV, USA). The rAAVs were injected bilaterally at a rate of 0.05 μl/min for 0.4 μl. The needle was left in place for 10 min after the end of the injection to ensure optimal diffusion. After surgery, each mouse was placed on a heat mat for a two-hour recovery before being returned to its home cage, and i.p. injections of Metacam® (2 mg/kg) were given for analgesia until the end of convalescence. Five to six weeks after shRNA injection, mice were sacrificed and NAc punches were dissected out for evaluation of *Grm4* expression using qRT-PCR, as described above. To check injection placement, two additional mice were deeply anesthetized as described above and transcardially perfused with a fixative [1% paraformaldehyde + 15% picric acid in 0.1 M phosphate buffer (PB), pH 7.2–7.4]. Brains were immediately removed from the skull and placed in ice-cold 0.1 M PB. Coronal 16-μm slices were cut using a cryostat (Leica CM1860; Leica Biosystems, Deer Park, IL, USA) and collected in PBS until performing anti-eGFP immunochemistry. Slices were washed in Tris-buffered saline (TBS), incubated with a rabbit polyclonal anti-eGFP primary antibody (Molecular Probes, Leiden, Netherlands, cat. no. A11122) diluted 1:1000 in a solution containing 2% normal goat serum (NGS), 0.2% Triton X-100 in TBS (TBS-T) for 72 h at 6°C with constant shaking. Slices were then washed in TBS (three times for 10 min) and incubated overnight (6°C) with a donkey Alexa 488-conjugated anti-rabbit secondary antibody (1:1000, Invitrogen, ThermoFisher Scientific, Waltham, MA, USA, cat. no. A32790) in TBS-T and 2% NGS. Slices were then extensively washed in TBS, mounted onto Superfrost Plus slides (Thermo Fisher Scientific, Waltham, MA, USA), and coverslipped with Vectashield (Vector Laboratory, Burlingame, CA, USA). Sections were imaged on Zeiss Imager Z.2 microscope (Zeiss, Oberkochen, Germany).

2.9.3. Grm4-targeting shRNA experiment in Fmr1$^{-/y}$ mice

Male *Fmr1*$^{-/y}$ mice were deeply anesthetized at the age of 8 weeks and placed on a stereotaxic frame, as described above. The stereotaxic injection of rAAVs (0.4×10^9 genome copies diluted in 0.01 M PBS) expressing either anti-*Grm4* shRNA or scramble shRNA was performed with a Hamilton syringe (Neuros 5 μl; Hamilton Company, Reno, NV, USA) in the NAc (coordinates from bregma: AP +1.4 mm; ML ±1.0 mm; DV −4.5 mm). The rAAVs were injected bilaterally at a rate of 0.05 μl/min for 0.4 μl. The needle was left in place for 10 min after the end of the injection to ensure optimal diffusion. After surgery, each mouse was placed on a heat mat for a two-hour recovery before being returned to its home cage, and i.p. injections of Metacam® (2 mg/kg) were given for analgesia until the end of convalescence. Mice recovered from the surgery for at least three weeks before behavioral assessment.

2.9.4. Behavioral experiments

Male *Fmr1*$^{-/y}$ mice were successively treated every four days with an acute sterile isotonic saline solution (NaCl 0.9%, i.p.), the mGlu4 PAM VU0155041 (10 mg/kg, i.p.) and the A2a adenosine receptor antagonist istradefylline (0.3 mg/kg, i.p.). Social behavior was assessed 30 min after each treatment using the direct social interaction test, as described above. At the end of experiments, mice were sacrificed and NAc brain punches were dissected out for assessment of *Grm4* transcript levels using qRT-PCR.

2.10. Statistics

Statistical analyses were performed using Statistica 9.0 software (StatSoft, Maisons-Alfort, France) or Prism 11.0.2 (GraphPad Software, Boston, MA, USA). For all comparisons, values of $p < 0.05$ were considered as significant. If normality of residuals was respected, statistical significance in behavioral experiments was assessed using two-way analysis of variance (followed by Tukey's post-hoc test in case of significant genotype x treatment interaction). In case of non-normality, we used the non-parametric Mann-Whitney *U* test or Kruskal-Wallis analysis of variance (followed by 2-tailed multiple comparison of mean ranks); consequently, genotype and treatment effects could not be interpreted in such two-factors experimental designs. In case of repeated or matched measures (i.e. time course of locomotor activity, stimulus in the three-chamber test, time and light conditions in photopharmacology, time in *Grm4*-targeting shRNA experiment, brain region in RNAscope® and qRT-PCR experiments), a repeated-measures three-way analysis of variance or a linear mixed-effects model including random intercepts for individual subjects, was performed followed by Tukey's post-hoc test when a significant interaction was detected. Unsupervised clustering analysis was performed on transformed qRT-PCR data [31,75] using complete linkage with correlation distance (Pearson correlation) for drug, treatment and brain region (Cluster 3.0 and Treeview software). Based on *a posteriori* multiple logistic regression (Table S2), principal component analysis (Figure S1) and principal component logistic regression (Table S3), both male and female groups showed similar behavior. Therefore, data of male and female subjects were pooled in the present study, except for the *Grm4*-targeting shRNA experiment in which only male *Fmr1*$^{-/y}$ mice were used.

3. Results

3.1. Altered striatal-dependent behaviors in *Fmr1*$^{-/-}$ mice

To test the hypothesis of altered striatal function in *Fmr1*$^{-/-}$ mice, we evaluated striatal-dependent behaviors. First, we assessed the stimulant locomotor effects of the dopamine D1/D5 dopamine receptor agonist SKF-81297 (s.c.; 0, 0.5, 1 and 2 mg/kg) and the inhibitory locomotor effects of low-to-moderate doses of the D2/D3 dopamine receptor agonist quinpirole (s.c.; 0, 0.05 and 0.1 mg/kg) in *Fmr1*$^{-/-}$ and *Fmr1*$^{+/+}$ mice (Fig. 1A). Consistent with previous reports [76,77], locomotor activity during habituation in both experiments was higher in *Fmr1*$^{-/-}$ mice as compared to *Fmr1*$^{+/+}$ mice. Under SKF-81297 administration, *Fmr1*$^{-/-}$ mice displayed increased locomotor response compared to *Fmr1*$^{+/+}$ mice, regardless of the dose. Both doses of quinpirole inhibited locomotion in *Fmr1*$^{+/+}$ mice for the first 30 min. However, this effect was maintained up to 60 min for the low dose (0.05 mg/kg) only (Figure S2), while the dose of 0.1 mg/kg may have shown a biphasic effect [62]. In contrast, quinpirole-induced suppression of locomotor activity was impaired in *Fmr1*$^{-/-}$ mice. Together, these results indicate that D1/D5 receptor agonist-induced activation is increased, whereas D2/D3 receptor activation is weaker in the absence of FMRP.

We then evaluated the cataleptic response induced by dopamine receptor antagonists, either targeting D1/D5 and D2/D3 receptors indifferently (haloperidol, 1 mg/kg), or targeting preferentially D1/D5 (SCH-23390, 0.3 mg/kg) or D2/D3 (sulpiride, 50 mg/kg) (Fig. 1B). Regardless of the molecule, *Fmr1*$^{-/-}$ mice spent less time in an unnatural position than *Fmr1*$^{+/+}$ mice. In contrast, when injected with a high dose of the opioid receptor agonist morphine (40 mg/kg), *Fmr1*$^{-/-}$ mice spent more time under cataleptic state than *Fmr1*$^{+/+}$ mice. Taken together, these results suggest a differential sensitivity of the striatum to dopamine receptor activation in *Fmr1*$^{-/-}$ versus *Fmr1*$^{+/+}$ mice.

3.2. Deficient social interaction and decreased number of Fos-positive D1-SPNs in the striatum of *Fmr1*$^{-/-}$ mice

Altered striatal-dependent behavior in *Fmr1*$^{-/-}$ mice could result from biased SPN balance of activity, a potential neurobiological substrate for impaired social behavior in this ASD model [31]. Here, we used RNAscope ISH to assess a marker of neuronal activity (*Fos* labelling) in D1-(*Pdyn* labelling) and D2-(*Penk* labelling) SPNs in the DS (medial and lateral) and NAc (Core and Shell) in *Fmr1*$^{-/-}$ and *Fmr1*$^{+/+}$ mice 45 min after a social interaction test (Fig. 2A).

Consistent with previous findings, *Fmr1*$^{-/-}$ mice displayed a severe deficit in social interaction (Figure 2B, S3A). RNAscope ISH revealed that the percentage of *Pdyn*$^{+}$-*Fos*$^{+}$ double-labelled cells (activated D1-SPNs) was reduced in the whole striatum of *Fmr1*$^{-/-}$ mice compared to *Fmr1*$^{+/+}$ mice. Meanwhile, the proportion of *Penk*$^{+}$-*Fos*$^{+}$ double-labelled cells (activated D2-SPNs) was found unchanged across striatal regions. Accordingly, the ratio of *Pdyn*$^{+}$-*Fos*$^{+}$ over *Penk*$^{+}$-*Fos*$^{+}$ labelled striatal cells was decreased in *Fmr1*$^{-/-}$ mice (Fig. 2C-D). Although the expression of both *Pdyn* and *Penk* was decreased in *Fmr1*$^{-/-}$ mice (Figure S4), the total number of *Pdyn*$^{+}$ or *Penk*$^{+}$ cells was similar (Figure S3B) indicating that neither the expression of SPN markers nor the total number of cells influenced the ratio of double-labelled cells. Altogether, these results suggest that the D1/D2-SPN balance of activity could be biased in *Fmr1*$^{-/-}$ mice and shifted towards deficient striatal D1-SPN activity following social interaction in these mice.

3.3. Rescued social behavior in *Fmr1*$^{-/-}$ mice under chronic facilitation of mGlu4 activity

Based on this SPN imbalance working hypothesis, we reasoned that treatment developed to decrease D2-SPN activity [43,46–48,50,53–56] such as a mGlu4 PAM would reverse their behavioral deficits. We first verified *in cellulo* that the absence of *Fmr1* in HEK293 cells does not affect the expression of G protein-coupled receptors and their coupling to G proteins. In *Fmr1*$^{-/-}$ cells, mGlu4 shows similar levels of expression and function as in *Fmr1*$^{+/+}$ HEK293 cells (Figure S5). In *Fmr1*$^{-/-}$ mice, *Grm4* mRNA expression was maintained compared to *Fmr1*$^{+/+}$ mice across several brain regions (Figure S4). We then evaluated the effects of chronically administering (D1 to D18) the mGlu4 PAM VU0155041 (0, 2.5 or 5 mg/kg) on ASD-like behavioral deficits in *Fmr1*$^{-/-}$ and *Fmr1*$^{+/+}$ mice (Fig. 3A).

We first focused on social behavior. In the direct social interaction test (Fig. 3B and Figure S6A), *Fmr1*$^{-/-}$ mice displayed a severe deficit that was reversed under chronic VU0155041 treatment, partially at the dose of 2.5 mg/kg, and fully at the dose of 5 mg/kg. When VU0155041 was administered only once, this 5 mg/kg dose produced only partial effects on social interaction (Figure S7). In the 3-chamber test for social preference (Fig. 3C and Figure S6B), *Fmr1*$^{-/-}$ mice failed to display preference for spending more time interacting with a congener over a toy. VU0155041 restored social preference from the lowest dose tested in *Fmr1*$^{-/-}$ mice. Together, these data indicate that facilitating mGlu4 activity alleviates social deficits in *Fmr1*$^{-/-}$ mice.

3.4. Normalized stereotypic behavior, anxiety, activity, catalepsy and cognition in *Fmr1*$^{-/-}$ mice under chronic facilitation of mGlu4 activity

We then assessed the effects of chronic VU0155041 on non-social ASD-related stereotypic motor behavior, perseveration and anxiety-like behavior in *Fmr1*$^{-/-}$ and *Fmr1*$^{+/+}$ mice [75–77].

Regarding spontaneous motor stereotypies, VU0155041 at both tested doses suppressed excessive grooming and circling in *Fmr1*$^{-/-}$ mice (Figure 3D and S6C). In the marble burying test, chronic VU0155041 administration abolished excessive marble burying in *Fmr1*$^{-/-}$ mice from the lowest dose (2.5 mg/kg) (Figure S6D). During Y-maze exploration, *Fmr1*$^{-/-}$ mice displayed reduced spontaneous alternation (SPA) rate and increased perseverative same arm re-entries (SAR) compared to *Fmr1*$^{+/+}$

mice. VU0155041 suppressed SAR and normalized SPA (at the highest dose) (Figure 3E and S6E). Finally, *Fmr1*$^{-/-}$ mice displayed longer latencies to eat and reduced food intake in the novelty-suppressed feeding test, suggesting increased levels of anxiety. Maximal efficiency of chronic VU0155041 in relieving this excessive anxiety was reached from the lowest dose (Fig. 3 F and S6F).

We then evaluated whether the beneficial effects of the optimal 5 mg/kg dose of VU0155041 administered chronically would generalize to other behavioral features in *Fmr1*$^{-/-}$ mice: locomotor hyperactivity, facilitated morphine-induced catalepsy, altered nociceptive thresholds and cognitive impairments [78,79] (Fig. 4A).

Regarding locomotion, we confirmed hyperactivity in vehicle-treated *Fmr1*$^{-/-}$ mice over 60 min. VU0155041 administration normalized activity in these mice to *Fmr1*$^{+/+}$ levels (Fig. 4B). As previously demonstrated (Fig. 1B), vehicle-treated *Fmr1*$^{-/-}$ mice exhibited longer catalepsy following morphine administration than *Fmr1*$^{+/+}$ mice; mGlu4 facilitation suppressed this difference (Fig. 4C). In the tail immersion test, VU0155041 increased nociceptive thresholds in both *Fmr1*$^{-/-}$ and *Fmr1*$^{+/+}$ mice, at 48°C. At 50°C, analgesia was only noticed in VU0155041-treated compared to vehicle-treated *Fmr1*$^{-/-}$ mice (Fig. 4D). Lastly, *Fmr1*$^{-/-}$ mice displayed a deficit both in detecting the change in location of an object and recognizing a novel object. Chronic VU0155041 failed to restore object location performance but fully rescued novel object recognition in these mice (Fig. 4E). These results indicate that the benefit of mGlu4 PAM administration exceeds ASD-like symptoms in *Fmr1*$^{-/-}$ mice and extend to other, more FXS-specific, behavioral comorbidities.

3.5. Beneficial behavioral effects in *Fmr1*$^{-/-}$ mice treated with different pharmacological compounds developed to dampen D2-SPN activity

To further explore the interest of facilitating mGlu4 activity to relieve behavioral deficits in *Fmr1*$^{-/-}$ mice, we evaluated the effects of chronic treatment with another mGlu4 PAM, ADX88178 (0, 5 or 10 mg/kg), and the orthosteric mGlu4 agonist LSP4–2022 [55] (0, 0.5 or 2 mg/kg). Moreover, we assessed the effects of a different compound developed to decrease D2-SPN activity, the A2a antagonist istradefylline [50] (0.3 mg/kg) (see timeline of experiments and more behavioral

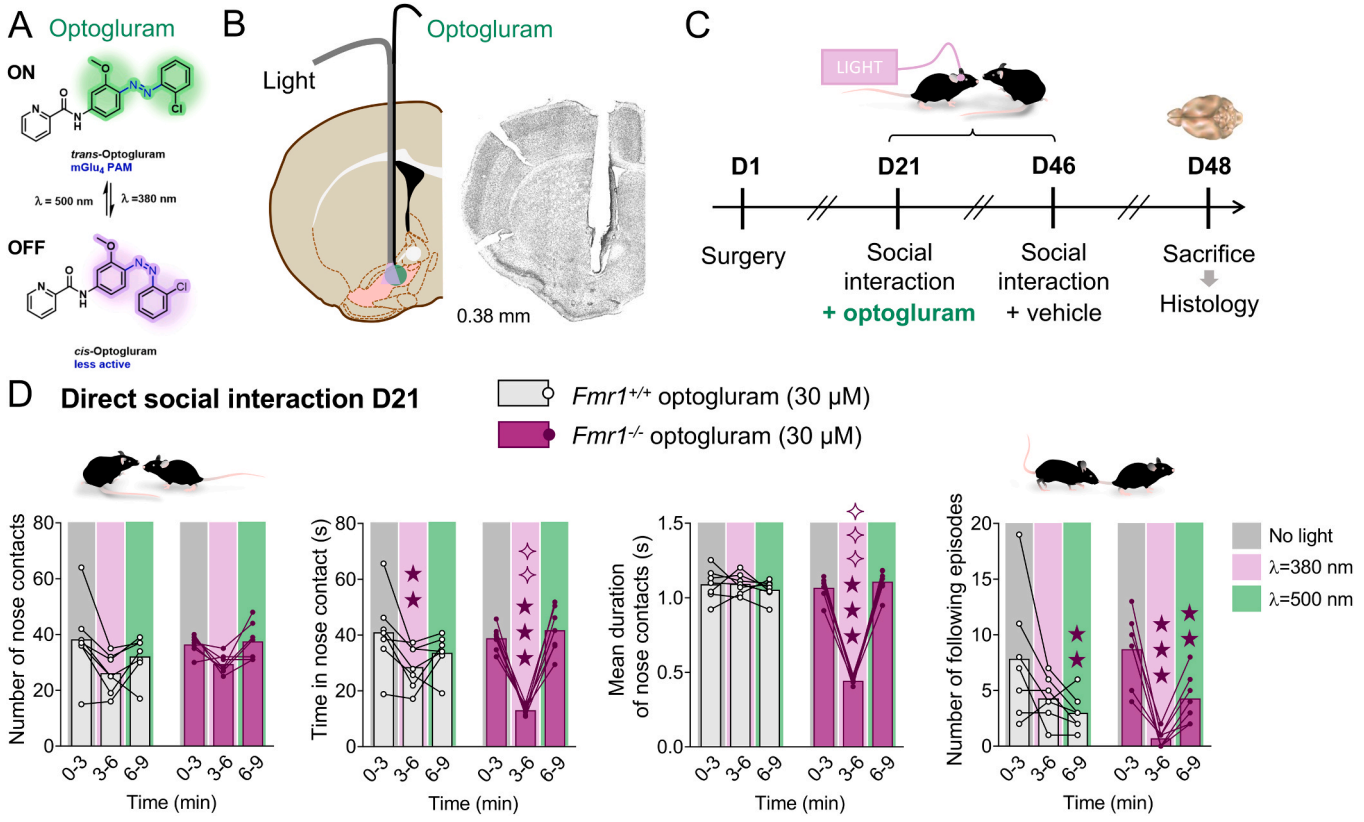


Fig. 6. Effects of photopharmacological activation within the ventral pallidum of the mGlu4 PAM optogluram on social interaction in *Fmr1*$^{-/-}$ mice. (A) The mGlu4 PAM optogluram can be switched from a trans-active configuration to a cis-inactive configuration after illumination with violet light (λ=380 nm) and from cis to trans with green light (λ=500 nm). (B) Scheme: a hybrid cannula for light and fluid delivery was positioned at the upper limit of VP. Picture: representative microphotograph showing cannula placement in the VP. Coordinates refer to bregma. Cannula placement for all mice was mapped on schematic brain sections in Fig. S9D. (C) A first social interaction session was performed in presence of optogluram at D21 following surgery (n = 7 mice per group). A second session was performed at D46 during which the vehicle of optogluram (NaCl 0.9%) was microinjected into the VP (Fig. S9C). Mice were sacrificed at D48 for verification of cannula placement. (D) In the direct social interaction test, under the no-light condition (0–3 min), optogluram was active and *Fmr1*$^{-/-}$ mice behaved similarly to *Fmr1*$^{+/+}$ mice. Illuminating optogluram with violet light (3–6 min) reduced the number of nose contacts regardless of the treatment and genotype (*A: $F_{2,24}$=10.9, $p < 0.001$*). This manipulation inactivated optogluram and reduced the time spent in nose contact in both *Fmr1*$^{+/+}$ and *Fmr1*$^{-/-}$ mice, but more severely in the latter. Green light, by reactivating optogluram (6–9 min), normalized the time of interaction in *Fmr1*$^{-/-}$ mice back to *Fmr1*$^{+/+}$ mice levels (*G x Tr x A: $F_{2,24}$=12.0, $p < 0.001$*). Inactivating optogluram markedly reduced the mean duration of nose contacts in *Fmr1*$^{-/-}$ mice, but not in *Fmr1*$^{+/+}$ mice—reactivating optogluram rescued this social parameter (*G x Tr x A: $F_{2,24}$=51.0, $p < 0.001$*). Switching off optogluram decreased the number of following episodes in *Fmr1*$^{-/-}$ mice (*G x Tr x A: $F_{2,24}$=4.4, $p < 0.05$*). Reactivation under green light tended to restore this behavior ($p = 0.062$), whereas a decrease in following episodes was noticed in *Fmr1*$^{+/+}$ animals. Results are shown as scatter plots, mean bars and individual before-after lines. Solid stars: comparison with the optogluram-treated group of the same genotype under the no-light condition; diamonds: comparison with the optogluram-treated *Fmr1*$^{+/+}$ group under the same light condition. One symbol: $p < 0.05$; two symbols: $p < 0.01$; three symbols: $p < 0.001$. Abbreviations: A: optogluram activation (on versus off); D: day; G: genotype; Tr: treatment (optogluram versus vehicle; vehicle data are displayed in Fig. S9C).

parameters in Figure S8).

Chronic administration of ADX88178 demonstrated similar efficiency as VU0155041 in relieving social behavior deficits, stereotypies, and perseveration in *Fmr1*$^{-/-}$ mice. In contrast, treatment with LSP4–2022 demonstrated beneficial effects at the low dose of 0.5 mg/kg only; at a higher dose (2 mg/kg), this compound not only failed to alleviate ASD-like behavior in *Fmr1*$^{-/-}$ mice but showed deleterious effects on social and perseverative behavior in *Fmr1*$^{+/+}$ mice, possibly by activating mGlu7 receptors [80]. Last of all, the A2a antagonist istradefylline (0.3 mg/kg) improved both social and repetitive behavior in *Fmr1*$^{-/-}$ mice (Fig. 5A-D). Overall, these results indicate that blocking the A2a receptor shows similar efficacy in alleviating ASD-like symptoms as facilitating mGlu4 activity with a higher dose of both PAMs, VU0155041 and ADX88178, or activating mGlu4 with a lower dose of the agonist LSP4–2022 (Figure S1).

3.6. Alleviated social deficits in *Fmr1*$^{-/-}$ mice under optical modulation of mGlu4 in the ventral pallidum

In previous experiments, mGlu4 PAMs/agonists were administered peripherally, targeting mGlu4 in the whole brain and organism. To better dissect the therapeutic effects in *Fmr1*$^{-/-}$ mice, we used photopharmacology to modulate mGlu4 activity in the VP, the main projection site of both NAc D1- and D2-SPNs. We injected optogluram, a light-

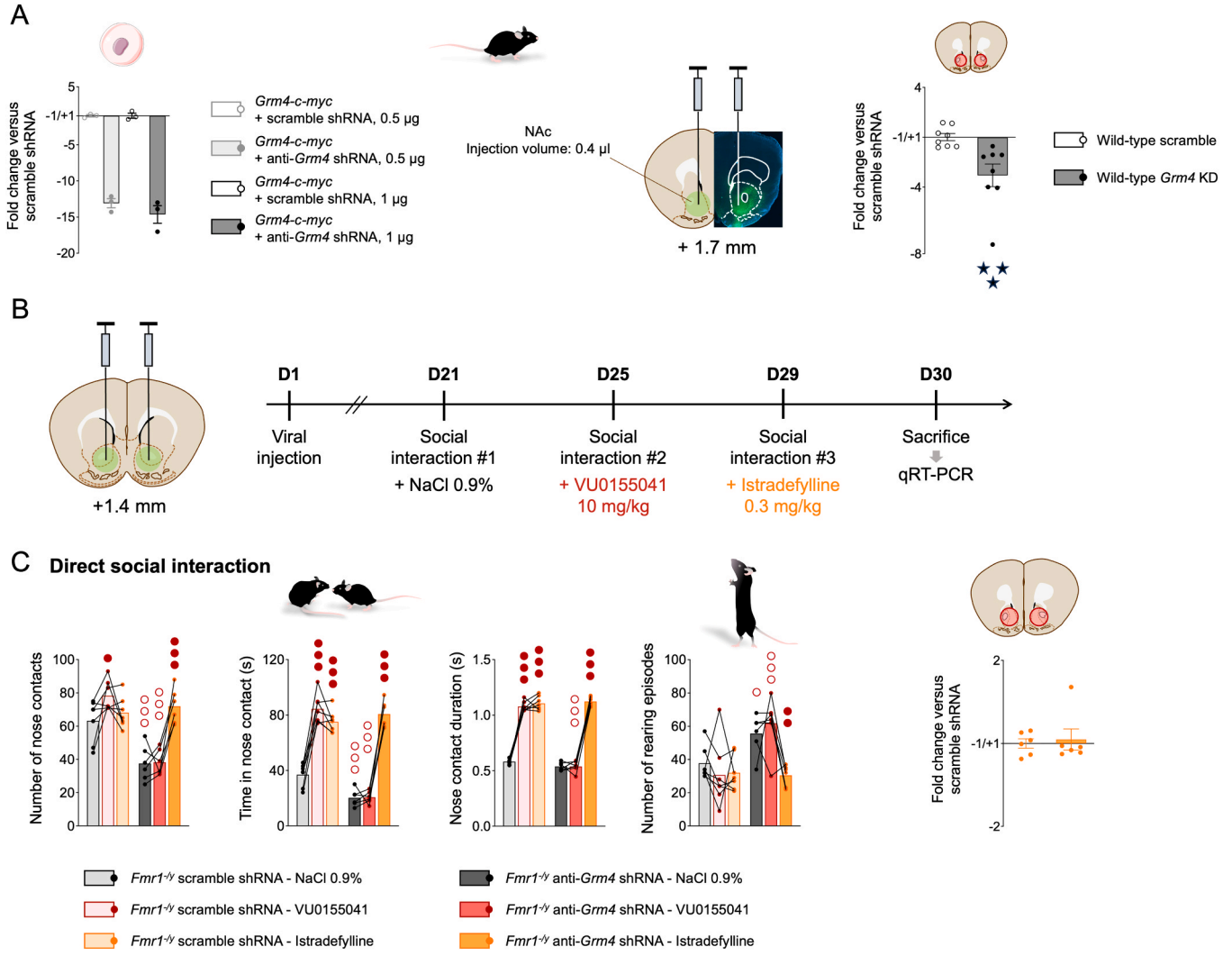


Fig. 7. Effects of a *Grm4*-targeting shRNA in the nucleus accumbens on social interaction in *Fmr1*$^{-/y}$ mice. (A) In the pilot experiment, the decrease of *Grm4* expression was first evaluated in HEK293FT co-transfected with mouse c-myc-tagged mGlu4 receptor and either 0.5 or 1 µg of eGFP-tagged anti-*Grm4* shRNA-expressing plasmid ($H_{3,12}$=8.6, $p < 0.01$). *Grm4* KD was then validated *in vivo* in the NAc of wild-type mice (U=2.5, $p < 0.001$). (B) A cohort of male *Fmr1*$^{-/y}$ mice was injected in the NAc with rAAVs expressing either an anti-*Grm4* or a scramble shRNA (n = 6–7 per group). At least three weeks after stereotaxic surgery, *Fmr1*$^{-/y}$ mice were successively treated with saline solution (NaCl 0.9%, i.p.), mGlu4 PAM VU0155041 (10 mg/kg, i.p.) and A2a adenosine receptor antagonist istradefylline (0.3 mg/kg, i.p.). Social behavior was assessed 30 min after each treatment. Mice were sacrificed after the third social interaction test for verification of *Grm4* expression in the NAc. (C) In the direct social interaction test, after saline treatment, NAc anti-*Grm4* shRNA decreased the number (*shRNA x Tr:* $F_{2,22}$=19.3, $p < 0.001$) and the time spent in nose contacts (*shRNA x Tr:* $F_{2,22}$=80.5, $p < 0.001$) as well as it increased rearing behavior (*shRNA x Tr:* $F_{2,22}$=4.8, $p < 0.05$). Under the scramble condition but not the *Grm4*-targeting one, the mGlu4 PAM VU0155041 increased the number (*shRNA x Tr:* $F_{2,22}$=19.3, $p < 0.001$), the time spent in (*shRNA x Tr:* $F_{2,22}$=80.5, $p < 0.001$) and the mean duration (*shRNA x Tr:* $F_{2,33}$=142.3, $p < 0.001$) of nose contacts. Finally, istradefylline restored all these parameters under the *Grm4*-targeting shRNA condition. *Grm4* KD was not detectable at transcript level in the NAc of *Fmr1*$^{-/y}$ mice (U=16.0, *NS*). Results are shown as scatter plots, mean bars and individual before-after lines. Black solid stars: comparison with the wild-type group; open circles: comparison with the scramble *Fmr1*$^{-/y}$ group under the same treatment condition; solid circles: comparison with the saline group under the same shRNA condition. One symbol: $p < 0.05$; two symbols: $p < 0.01$; three symbols: $p < 0.001$. Abbreviations: D: day; eGFP: enhanced green fluorescent protein; KD: knockdown; NAc: nucleus accumbens; NS: not significant; rAAV: recombinant adeno-associated virus; shRNA: short hairpin RNA; Tr: treatment.

sensitive mGlu4 PAM [81], in this region, through a cannula coupled with an optic fiber. We controlled optogluram activity by switching it from active (resting) to inactive (violet light, 380 nm) state, then back to active state (green light, 500 nm) (Fig. 6A, B). After 3 weeks of post-surgery recovery, social behavior was assessed in *Fmr1*$^{+/+}$ and *Fmr1*$^{-/-}$ mice using the direct social interaction test (Fig. 6C). After another 3 weeks, all the mice underwent the same protocol after intra-VP injection of vehicle, to assess the effects of light *per se* (micro-injection of optogluram vehicle, Figure S9C).

During the 3-min baseline, when the light was off and optogluram active, *Fmr1*$^{-/-}$ mice displayed normalized social behavior. When violet light (380 nm) was switched on and optogluram inactivated (3–6 min), a significant deficit in social interaction became detectable in *Fmr1*$^{-/-}$ mice, which was completely rescued under green light (500 nm) and reactivation of optogluram (6–9 min) (Figures 6D and S9B). Switching on and off optogluram reduced the time spent in nose contact in *Fmr1*$^{+/+}$ mice, without effect on mean duration of nose contacts. Moreover, neither green or violet light in the absence of optogluram influenced behavior in *Fmr1*$^{+/+}$ and *Fmr1*$^{-/-}$ mice (Figure S9C). Thus, facilitating the activity of mGlu4 in the VP is sufficient to restore social abilities in *Fmr1*$^{-/-}$ mice.

3.7. Role of NAc mGlu4 in relieving social deficits in *Fmr1*$^{-/y}$ mice

Since mGlu4 expression in the VP is not restricted to NAc SPN terminals [44,45,81–85], we aimed to evaluate the specific requirement of NAc mGlu4 in relieving social deficits.

Once validated *Grm4* knockdown (KD) in HEK cells and in the NAc of wild-type mice (Fig. 7A), we injected rAAVs expressing either an anti-*Grm4* or a scramble shRNA in the NAc of *Fmr1*$^{-/y}$ mice and assessed social interaction after saline (NaCl 0.9%, i.p.), mGlu4 PAM VU0155041 (10 mg/kg, i.p.) or A2a antagonist istradefylline (0.3 mg/kg, i.p.) peripheral administration (Fig. 7B). In *Fmr1*$^{-/y}$ mice, *Grm4*-targeting shRNA decreased social interaction, while increasing non-social directed exploration, suggesting a contribution of NAc mGlu4 to these behaviors (Fig. 7C). Most remarkably, mGlu4 PAM treatment failed to restore social behavior in *Fmr1*$^{-/y}$ mice, indicating that mGlu4 receptors expressed in NAc cells could contribute to the relieving effects of systemic mGlu4 PAM treatment (Fig. 7C and Figure S10). In contrast, istradefylline was still able to relieve social deficits, showing that acting on another pharmacological target, enriched in D2-SPNs, was sufficient to improve social behavior in *Fmr1*$^{-/y}$ mice.

Grm4 KD was not detectable at transcript level in the NAc of *Fmr1*$^{-/y}$ mice, whilst it was validated at transcript level in *Grm4*-overexpressing heterologous cells and *ex vivo* in wild-type animals. Intriguingly, current literature reporting on KD in *Fmr1* knockout models does not display any transcriptional validation methods, as usually performed, but mentions alternative assays, which raises questions about RNA interference mechanisms in FXS mouse models [86–89]. FMRP is known to interact with several components of the RNA silencing ribonucleoprotein complex to repress protein translation [86,90–94]. However, this FMRP-dependent mechanism remains elusive and FMRP deficiency does not necessarily prevent the effects of RNA-induced silencing in cells, including in brain cells from *Fmr1*$^{-/-}$ mice [86–88,93]. Moreover, RNA-induced silencing was previously shown to regulate behavior in *Fmr1*$^{-/-}$ mice [89], consistent with behavioral data in the present study showing a significant effect of *Grm4*-targeting shRNA in the NAc of *Fmr1*$^{-/y}$ mice, including under vehicle treatment.

4. Discussion

FXS is currently the leading monogenic cause of ASD [4]. The striatum plays a key role in the ASD-like phenotype [23,25]. To date, clinical [95,96] and preclinical studies [97–100] investigating striatal dysfunction in FXS have mainly focused on the DS and its cortical afferences. However, social withdrawal, reward deficit, repetitive behaviors, and lack of flexibility in FXS and its *Fmr1*$^{-/-}$ mouse model [4,21] point towards ventral striatal dysfunction [22,29–35]. Consistent with this, altered physiology and connectivity of D1- and D2-SPNs have been evidenced in the NAc of *Fmr1*$^{-/-}$ mice [38–41]. In the present study, we interrogated a potential imbalance of D1/D2-SPN activity in *Fmr1*$^{-/-}$ mice, notably in the NAc, and its potential therapeutic implications for the management of ASD symptomatology.

We first assessed the locomotor effects of dopaminergic agonists in *Fmr1*$^{-/-}$ mice, as a proxy of striatal function. The D1/D5 receptor agonist SKF-81297 dose-dependently produced hyperlocomotion in mice, and this hyperlocomotion was more pronounced in *Fmr1*$^{-/-}$ mice, consistent with increased mEPSC and synaptic contacts at dorsolateral D1-SPNs in *Fmr1*$^{-/-}$ mice [100]. In contrast, low doses of the D2/D3 receptor agonist quinpirole inhibited locomotion less in *Fmr1*$^{-/-}$ mice than in their *Fmr1*$^{+/+}$ controls. At low doses, quinpirole was reported to reduce locomotion in mice [62,101,102]. This inhibition would mainly result from the activation of D2 presynaptic and/or somatodendritic autoreceptors at mesencephalic DA neurons and the subsequent decrease in striatal DA release [102–104]. In *Fmr1*$^{-/-}$ mice, although *Drd2* expression was not regulated in either the VTA or striatum (Figure S4), an increase in striatal D2 receptor density was reported [105]. Besides, increasing D2 receptor expression in NAc Core D2-SPNs is sufficient to increase ambulatory behavior in mice [106]. Thus, an increase of somatodendritic D2 receptor density in the NAc of *Fmr1*$^{-/-}$ mice may have reduced the efficacy of low doses of D2 receptor agonist. We then explored catalepsy in *Fmr1*$^{-/-}$ mice. The cataleptic response to D1/D5 and D2/D3 receptor antagonists was reduced in *Fmr1*$^{-/-}$ mice, possibly a consequence of locomotor hyperactivity in *Fmr1*$^{-/-}$ mice [76,77]. Conversely, akinetic and cataleptic effects of morphine were increased in *Fmr1*$^{-/-}$ mice, indicating an increased morphine-induced response of the NAc, where the *Oprm1* gene, coding for mu opioid receptor, is enriched and expressed in both types of SPNs [107–109]. A2a receptor antagonists reduce morphine-induced catalepsy [110,111], likely by reducing NAc D2-SPN activity [50], which indirectly suggests a biased SPN balance of activity in *Fmr1*$^{-/-}$ mice.

We then used RNAscope® to assess this balance of activity post-mortem in *Fmr1*$^{-/-}$ mice, following a social encounter. We demonstrated that the proportion of *Pdyn-Fos*-positive neurons, namely active D1-SPNs, was lower in the striatum, DS and NAc, of *Fmr1*$^{-/-}$ mice compared to *Fmr1*$^{+/+}$ mice, resulting in decreased *Pdyn/Penk-Fos*-positive ratio. This modification of the ratio was not due to neuronal loss or change in the expression of SPN markers, since the total number of *Pdyn*-positive SPNs was maintained and both *Pdyn* and *Penk* expression were decreased in *Fmr1*$^{-/-}$ mice. Whether this decrease would be less pronounced in the DS compared to NAc will need further investigation, with more statistical power. Our finding of decreased *Fos*-labelled D1-SPNs, notably in the NAc, matches recent report of decreased D1-SPN intrinsic excitability, but increased D2-SPN intrinsic excitability, in NAc Core slices of *Fmr1*$^{-/-}$ mice [40]. One might propose that such changes would result from compensatory mechanisms in response to protein expression dysregulations (e.g. dopamine receptors) in the absence of FMRP [100,105]. Either way, modifications in SPN excitability likely involve modified synaptic transmission within cortico- and amygdalo-striatal circuits, and notably increased synaptic strength within the BLA/PFC to NAc Core pathways [41,100]. NAc D2-SPNs were shown to play a critical role in controlling social behavior. Their activation in naive mice makes them more susceptible to social stress, and socially defeated mice, which display social avoidance, show increased NAc D2-SPN activity [34]. Accordingly, an overweight of NAc D2-SPN outputs, resulting either from reduced NAc D1-SPN outputs or from direct stimulation of NAc D2-SPNs, induces social avoidance, while activating NAc D1-SPNs facilitates social behavior [31,32,34–36,112]. Hence, we and others propose a model in which an imbalance in NAc SPN activity biased towards D2-SPNs contributes to the social deficits of *Fmr1*$^{-/-}$ mice [24,25,31,32]. Thus, decreasing D2-SPN activity should be a promising therapeutic option [31,32].

Consistent with this hypothesis, treating *Fmr1*$^{-/-}$ mice chronically with pharmacological compounds that were developed to decrease D2-SPN activity [43,46–48,50,53–56] relieved their ASD-like behavioral deficits. Here, the mGlu4 PAMs VU0155041 and ADX88178 restored social interaction and social preference in a dose-dependent manner and reduced stereotypic and perseverative behaviors in *Fmr1*$^{-/-}$ mice. The orthosteric mGlu4 agonist LSP4–2022 produced similar beneficial effects, but at low dose only, when more selectively recruiting mGlu4 [55]. Thus, facilitating mGlu4 signaling rescues ASD-like behavior in *Fmr1*$^{-/-}$ mice, as previously shown in this model [51].

Besides its effects on ASD-like deficits, enhancing mGlu4 activity with VU0155041 reduced hyperactivity, anxiety-like behaviors, normalized morphine-induced catalepsy, showed analgesic effects and restored novel object recognition (but not object location) in *Fmr1*$^{-/-}$ mice. Such effects may involve a widespread action of the drug at cerebral mGlu4 after systemic administration, within corticostriatal projections [44,113], hippocampus, entorhinal cortex, thalamic nuclei [44,114] and amygdala and/or spinal cord [81,115], in addition to the cerebellum [51]. The therapeutic potential of mGlu4 facilitators thus extends beyond the diagnostic symptoms of ASD in FXS, to comorbid conditions such as hyperactivity, and cognitive deficits.

When used at a high dose (2 mg/kg), recruiting mGlu7 in addition to mGlu4, the agonist LSP4–2022 showed no effect on social interaction and only partial benefit on social preference in *Fmr1*$^{-/-}$ mice, but a deleterious impact on social behavior in *Fmr1*$^{+/+}$ mice. This result suggests that activating mGlu7 may be inefficient to relieve social deficit in *Fmr1*$^{-/-}$ mice, in contrast with positive outcomes on protein synthesis and cognitive performance [116]. However, the mGlu7 PAM VU0422288 improved social preference and cognitive abilities in the *Mecp2* heterozygous (*Mecp2*$^{+/-}$) mouse model of Rett syndrome, which displays reduced levels of mGlu7 protein expression [117]. Intriguingly, VU0422288 also behaves as a potent mGlu4 PAM [118], suggesting that a delicate interplay between mGlu4 and mGlu7 signaling may intervene in the control of social behavior, as proposed for motor control [45]. Further investigations are required to comprehensively explore the therapeutic potential of targeting mGlu7 in mouse models of ASD.

Finally, chronically administered A2a antagonist istradefylline normalized ASD-like behaviors in *Fmr1*$^{-/-}$ mice similarly to mGlu4 facilitators/activators. Istradefylline was previously found to improve novel object recognition and hippocampal function in *Fmr1*$^{-/-}$ mice [52]. Positive effects on social behavior have likely involved istradefylline-mediated inhibition of D2-SPNs, in which A2a receptor expression is highly enriched [49,50], as for mice bearing a specific ablation of NAc D1-SPNs [31]. Although post-mortem assessment of neuronal activity (RNAscope® experiments) and systemic administration of pharmacological compounds do not allow to conclude for a specific contribution of D2-SPN inhibition, this set of results converges towards a potential role of NAc SPNs in relieving ASD-like deficits in FXS.

Based on high expression of mGlu4 in the cerebellum [44,82] and improved cerebellum-dependent behavioral responses in VU0155041-treated *Fmr1*$^{-/-}$ mice [51], Martín et al. proposed that positive effects of mGlu4 facilitation on social behavior may involve cerebellar mGlu4. In the present study, photopharmacological facilitation of mGlu4 in the VP, together with *Grm4*-targeting shRNA experiment in the NAc, points towards a potential regulatory role of mGlu4 receptors located on NAc SPN terminals on social behavior in *Fmr1*$^{-/-}$ mice, but further studies are needed to confirm this. In the VP, mGlu4 expression is restricted to afferent terminals, although it is likely not limited to D2-SPNs [44,45,81–85]. However, most mGlu4-positive staining in the VP is found on axon terminals forming symmetrical synapses, which are considered GABAergic [44], suggesting the contribution of NAc SPN mGlu4 receptors to the beneficial effects of optogluram. In addition, targeting *Grm4* with shRNA in NAc cells is sufficient to alter social behavior and to prevent the social-relieving effects of systemic mGlu4 PAM administration in *Fmr1*$^{-/y}$ mice. Since mGlu4 is only weakly expressed by striatal cells other than SPNs [85,119,120], literature data and the present findings suggest that NAc SPN mGlu4 receptors could modulate social behavior. Importantly, mGlu4 is expressed in both D1- and D2-SPNs [44,82,85], and has been proposed to reduce D2-SPN output through actions at corticostriatal terminals [113], D1-SPN-CIN synapses [121,122] and D2-SPN projections to the VP [43,46,48]. Positive allosteric modulation of mGlu4 prevented tardive dyskinesias in Parkinson's disease models [43,47] and rescued social deficits induced by NAc D1-SPN ablation or sustained NAc D2-SPN optoactivation [31]. mGlu4 PAM also restored social behavior in morphine-abstinent mice [42], which display excessive D2-SPN activity [123], and in the *Oprm1*$^{-/-}$ ASD-like model, characterized by reduced NAc *Grm4* expression [75,124,125]. Together, literature data and the present findings point towards a model in which facilitating mGlu4 activity may alleviate ASD-like symptoms by decreasing D2-SPN activity, particularly in the NAc; however, further studies are required to establish the validity of this proposed mechanism.

Based on this working hypothesis and findings of other studies, restoration of social behavior is likely to involve inhibition of NAc D2-SPNs, while reduced stereotypies may result from inhibition of D2-SPN populations in the dorsomedial, central and ventral striatum (i.e. NAc) [31,32,126,127]. However, the imbalance between SPN activity appears to be reversed in the dorsolateral striatum of *Fmr1*$^{-/-}$ mice, in which D1-SPN excitability was reported to be increased and correlated with repetitive behaviors [100]. Thus, a finely tuned balance SPN activity likely contributes to control motor behaviors in different subregions of the DS [128,129].

Finally, photopharmacological experiments highlight the involvement of VP in controlling social interaction in *Fmr1*$^{-/-}$ mice. Besides, relieving effects of mGlu4 PAM on social deficits induced by NAc D1-SPN ablation were associated with marked transcriptional down-regulation in the VP [31]. In this region, a finely tuned balance of activity between GABAergic and glutamatergic neuronal populations controls approach and avoidance behaviors, including social behaviors, in tight connection to the NAc D1/D2-SPN balance [33,130–133]. Interestingly, social avoidance triggered by optogenetic stimulation of D2-SPNs in mice was associated with increased *Fos* expression in the VP, suggesting increased neuronal activity consistent with electrophysiological studies [31,33]. Thus, emerging evidence suggests that the VP, a major node of the basal ganglia circuit, plays a crucial role in controlling social behavior.

In conclusion, our study pinpoints, under ASD-relevant behavioral conditions, a biased D1/D2-SPN balance in *Fmr1*$^{-/-}$ mice as well as a potential contribution of mGlu4 receptors located in the VP and *Grm4* in the NAc to the relieving effects of systemic mGlu4 PAMs in this model. Furthermore, it demonstrates the therapeutic potential of drugs developed to dampen D2-SPN activity to relieve ASD core symptoms but also co-morbidities of FXS.

Limitations and perspectives

Although our findings point towards a possible imbalance between D1- and D2-SPN pathways and suggest a contribution of NAc mGlu4 receptors to the regulation of social behavior in *Fmr1*$^{-/-}$ mice, several questions remain to be addressed with future investigations in order to fully validate the hypothesis.

First, SPN imbalance in the *Fmr1*$^{-/-}$ mouse model will require further characterization. Notably, the detected reduction in *Fos*$^{+}$ D1-SPN numbers may reflect diminished recruitment during social interaction, an intrinsic genotype-related alteration in activity-dependent plasticity, or a combination of both, which would imply broad effects on behavior, beyond the social repertoire. Regarding the effects of mGlu4 facilitation, whether this pharmacological manipulation allows normalizing the D1-/D2-SPN output balance remains to be investigated, to better link striatofugal imbalance to the social deficits displayed by *Fmr1*$^{-/-}$ mice. Considering mGlu4 location at SPN terminals, however, modified circuit

activity may instead affect downstream structures.

Second, additional experiments will be needed to clarify the role of NAc mGlu4 receptors. We injected a *Grm4*-targeting shRNA in the NAc of *Fmr1*$^{-/-}$ mice that abolished the effects of a systemic mGlu4 PAM but could not be confirmed the KD at RNA level, requiring cautious interpretation. Similar experiments in wild-type mice would provide a better understanding of the role of NAc mGlu4 in controlling social behavior. Furthermore, additional investigations are required to disentangle the respective roles of NAc D1- and D2-SPN mGlu4 receptor populations, using cell-specific optogenetic or chemogenetic manipulations in wild-type mice and ASD-like models—preferably not in a FMRP-null context, to circumvent interpretational challenges arising from uncontrolled alterations in the expression of genetic tools. Monitoring ventral pallidal neuronal activity, either in real time or using post-mortem activity markers, may help clarify how NAc D1- and D2-SPNs and their mGlu4 receptors modulate social behavior.

Finally, although the present study does not provide a complete cellular and molecular validation of the proposed mechanisms, behavioral and pharmacological findings collectively support the translational potential of mGlu4 modulation. Of note, while acute mGlu4 PAM treatment produced partial effects, chronic treatment allowed a full and broad behavioral recovery in *Fmr1*$^{-/-}$ mice, suggesting that longer-lasting adaptive or plasticity-related processes were recruited. Identifying such mechanisms will be important to better delineate the therapeutic potential of mGlu4-targeting compounds.

CRediT authorship contribution statement

Mathieu Fonteneau: Writing – review & editing, Writing – original draft, Visualization, Validation, Supervision, Project administration, Methodology, Investigation, Formal analysis, Data curation, Conceptualization. **Claire Terrier:** Writing – review & editing, Writing – original draft, Methodology, Investigation, Formal analysis, Data curation, Conceptualization. **Florian Bolot:** Writing – review & editing, Visualization, Formal analysis, Data curation. **Fani Pantouli:** Writing – review & editing, Methodology, Investigation, Formal analysis, Data curation. **Agathe Brugoux:** Writing – review & editing, Investigation, Formal analysis. **Fanny Malhaire:** Writing – review & editing, Methodology, Investigation, Formal analysis, Data curation. **Ingrid Wagnon:** Writing – review & editing, Investigation, Formal analysis. **Roser Borràs-Tuduri:** Writing – review & editing, Resources. **Paola Rossolillo:** Writing – review & editing, Resources, Methodology. **Isabelle McCort-Tranchepain:** Writing – review & editing, Resources. **Alexis Bailey:** Writing – review & editing, Supervision, Funding acquisition. **Francine Acher:** Writing – review & editing, Supervision, Resources, Funding acquisition. **Amadeu Llebaria:** Writing – review & editing, Supervision, Resources, Funding acquisition. **Cyril Goudet:** Writing – review & editing, Supervision, Methodology, Funding acquisition, Conceptualization. **Jérôme A.J. Becker:** Writing – review & editing, Writing – original draft, Visualization, Validation, Supervision, Project administration, Methodology, Investigation, Funding acquisition, Formal analysis, Data curation, Conceptualization. **Julie Le Merrer:** Writing – review & editing, Writing – original draft, Visualization, Validation, Supervision, Project administration, Methodology, Investigation, Funding acquisition, Formal analysis, Data curation, Conceptualization.

Ethics declaration

This study was conducted in accordance with the ARRIVE (Animal Research: Reporting of In Vivo Experiments) guidelines. This study was approved by the Comité d'Éthique en Expérimentation Animale Val de Loire. (Approval No. APAFIS#57856–2025111817283407 and APAFIS#27791–2020102017528289)

Funding

This study was supported by the French National Research Agency (ANR-17-NEU3–0001, as part of Neuron Cofund ERA-NET program, and ANR-21-CE18–0040). FP received support from the British Society for Neuroendocrinology. CT acknowledges support from the ERA-NET Neuron program. This work received support from the Institut National de la Santé et de la Recherche Médicale (Inserm), Centre National de la Recherche Scientifique (CNRS), Institut National de Recherche pour l'Agriculture, l'Alimentation et l'Environnement (INRAe) and Université de Tours.

Declaration of Competing Interest

The authors declare that they have no known competing financial interests or personal relationships that could have appeared to influence the work reported in this paper.

Acknowledgments

We acknowledge the technical assistance of Drs. Jorge Gandia and Thibaut Laboute, Yannick Corde, Audrey Léauté and Déborah Jaccaz in performing experiments. We thank Pascale Koebel for shRNA design and rAAV production. We acknowledge Pr. Ingrid Erlich for technical advising and training on eGFP immunostaining as well as Frédéric Briend for statistical help. We thank the Experimental Unit PAO-1297 (EU0028, Animal Physiology Experimental Facility, DOI: 10.15454/1.5573896321728955E12) from the INRAe-Val de Loire Centre for animal breeding and care. Cell-based pharmacology assays were performed at the ARPEGE (Pharmacology Screening-Interactome) platform facility at the Institut de Génomique Fonctionnelle (Montpellier). We thank Drs. Xavier Rovira and Xavier Gomez-Santacana at MCS (IQAC-CSIC) and Drs. Carme Serra and Lourdes Muñoz at SimChem (IQAC-CSIC) for compound design and synthesis.

Appendix A. Supporting information

Supplementary data associated with this article can be found in the online version at doi:10.1016/j.phrs.2026.109712.

Data availability

Data will be made available on request.

References

[1] American Psychiatric Association, Diagnostic and statistical manual of mental disorders: DSM-5, American Psychiatric Association, 2013.
[2] G. Ramaswami, D.H. Geschwind, Genetics of autism spectrum disorder, Handb. Clin. Neurol. 147 (2018) 321–329, https://doi.org/10.1016/B978-0-444-63233-3.00021-X.
[3] V.B. Searles Quick, B. Wang, M.W. State, Leveraging large genomic datasets to illuminate the pathobiology of autism spectrum disorders, Neuropsychopharmacology 46 (2021) 55–69, https://doi.org/10.1038/s41386-020-0768-y.
[4] R.J. Hagerman, E. Berry-Kravis, H.C. Hazlett, D.B. Bailey, H. Moine, R.F. Kooy, F. Tassone, I. Gantois, N. Sonenberg, J.L. Mandel, P.J. Hagerman, Fragile X syndrome, Nat. Rev. Dis. Prim. 3 (2017) 17065, https://doi.org/10.1038/nrdp.2017.65.
[5] W.E. Kaufmann, S.A. Kidd, H.F. Andrews, D.B. Budimirovic, A. Esler, B. Haas-Givler, T. Stackhouse, C. Riley, G. Peacock, S.L. Sherman, W.T. Brown, E. Berry-Kravis, Autism Spectrum Disorder in Fragile X Syndrome: Cooccurring Conditions and Current Treatment, Pediatrics 139 (2017) S194–S206, https://doi.org/10.1542/peds.2016–1159 F.
[6] A. McDuffie, L. Abbeduto, P. Lewis, S. Kover, J.S. Kim, A. Weber, W.T. Brown, Autism spectrum disorder in children and adolescents with fragile X syndrome: within-syndrome differences and age-related changes, Am. J. Intellect. Dev. Disabil. 115 (2010) 307–326, https://doi.org/10.1352/1944-7558-115.4.307.
[7] M.J. Salcedo-Arellano, B. Dufour, Y. McLennan, V. Martinez-Cerdeno, R. Hagerman, Fragile X syndrome and associated disorders: Clinical aspects and pathology, Neurobiol. Dis. 136 (2020) 104740, https://doi.org/10.1016/j.nbd.2020.104740.

[8] D. Protic, R. Hagerman, State-of-the-art therapies for fragile X syndrome, Dev. Med. Child. Neurol. 66 (2024) 863–871, https://doi.org/10.1111/dmcn.15885.
[9] G. Dolen, E. Osterweil, B.S. Rao, G.B. Smith, B.D. Auerbach, S. Chattarji, M. F. Bear, Correction of fragile X syndrome in mice, Neuron 56 (2007) 955–962, https://doi.org/10.1016/j.neuron.2007.12.001.
[10] A. Michalon, M. Sidorov, T.M. Ballard, L. Ozmen, W. Spooren, J.G. Wettstein, G. Jaeschke, M.F. Bear, L. Lindemann, Chronic pharmacological mGlu5 inhibition corrects fragile X in adult mice, Neuron 74 (2012) 49–56, https://doi.org/10.1016/j.neuron.2012.03.009.
[11] E.A. Youssef, E. Berry-Kravis, C. Czech, R.J. Hagerman, D. Hessl, C.Y. Wong, M. Rabbia, D. Deptula, A. John, R. Kinch, P. Drewitt, L. Lindemann, M. Marcinowski, R. Langland, C. Horn, P. Fontoura, L. Santarelli, J.A. Quiroz, FragXis Study Group, Effect of the mGluR5-NAM Basimglurant on Behavior in Adolescents and Adults with Fragile X Syndrome in a Randomized, Double-Blind, Placebo-Controlled Trial: FragXis Phase 2 Results, Neuropsychopharmacology 43 (2018) 503–512, https://doi.org/10.1038/npp.2017.177.
[12] E. Berry-Kravis, V. Des Portes, R. Hagerman, S. Jacquemont, P. Charles, J. Visootsak, M. Brinkman, K. Rerat, B. Koumaras, L. Zhu, G.M. Barth, T. Jaecklin, G. Apostol, F. von Raison, Mavoglurant in fragile X syndrome: Results of two randomized, double-blind, placebo-controlled trials, 321ra5, Sci. Transl. Med. 8 (2016), https://doi.org/10.1126/scitranslmed.aab4109.
[13] J.C. Darnell, S.J. Van Driesche, C. Zhang, K.Y. Hung, A. Mele, C.E. Fraser, E. F. Stone, C. Chen, J.J. Fak, S.W. Chi, D.D. Licatalosi, J.D. Richter, R.B. Darnell, FMRP stalls ribosomal translocation on mRNAs linked to synaptic function and autism, Cell 146 (2011) 247–261, https://doi.org/10.1016/j.cell.2011.06.013.
[14] K.M. Huber, S.M. Gallagher, S.T. Warren, M.F. Bear, Altered synaptic plasticity in a mouse model of fragile X mental retardation, Proc. Natl. Acad. Sci. USA 99 (2002) 7746–7750, https://doi.org/10.1073/pnas.122205699.
[15] R. Tabet, E. Moutin, J.A. Becker, D. Heintz, L. Fouillen, E. Flatter, W. Krezel, V. Alunni, P. Koebel, D. Dembele, F. Tassone, B. Bardoni, J.L. Mandel, N. Vitale, D. Muller, J. Le Merrer, H. Moine, Fragile X Mental Retardation Protein (FMRP) controls diacylglycerol kinase activity in neurons, E3619-28, Proc. Natl. Acad. Sci. USA 113 (2016), https://doi.org/10.1073/pnas.1522631113.
[16] H.G.S. Martin, O. Lassalle, J.T. Brown, O.J. Manzoni, Age-Dependent Long-Term Potentiation Deficits in the Prefrontal Cortex of the Fmr1 Knockout Mouse Model of Fragile X Syndrome, Cereb. Cortex 26 (2016) 2084–2092, https://doi.org/10.1093/cercor/bhv031.
[17] M.G. Haberl, V. Zerbi, A. Veltien, M. Ginger, A. Heerschap, A. Frick, Structural-functional connectivity deficits of neocortical circuits in the Fmr1 (-/y) mouse model of autism, Sci. Adv. 1 (2015) e1500775, https://doi.org/10.1126/sciadv.1500775.
[18] N. Kourdougli, A. Suresh, B. Liu, P. Juarez, A. Lin, D.T. Chung, A. Graven Sams, M.J. Gandal, V. Martinez-Cerdeno, D.V. Buonomano, B.J. Hall, C. Mombereau, C. Portera-Cailliau, Improvement of sensory deficits in fragile X mice by increasing cortical interneuron activity after the critical period, e6, Neuron 111 (2023) 2863–2880, https://doi.org/10.1016/j.neuron.2023.06.009.
[19] C. Bostrom, S.Y. Yau, N. Majaess, M. Vetrici, J. Gil-Mohapel, B.R. Christie, Hippocampal dysfunction and cognitive impairment in Fragile-X Syndrome, Neurosci. Biobehav. Rev. 68 (2016) 563–574, https://doi.org/10.1016/j.neubiorev.2016.06.033.
[20] J.A. Ronesi, K.A. Collins, S.A. Hays, N.P. Tsai, W. Guo, S.G. Birnbaum, J.H. Hu, P. F. Worley, J.R. Gibson, K.M. Huber, Disrupted Homer scaffolds mediate abnormal mGluR5 function in a mouse model of fragile X syndrome, S1, Nat. Neurosci. 15 (2012) 431–440, https://doi.org/10.1038/nn.3033.
[21] L.M. Schmitt, A.L. Arzuaga, A. Dapore, J. Duncan, M. Patel, J.R. Larson, C. A. Erickson, J.A. Sweeney, M.E. Ragozzino, Parallel learning and cognitive flexibility impairments between Fmr1 knockout mice and individuals with fragile X syndrome, Front. Behav. Neurosci. 16 (2022) 1074682, https://doi.org/10.3389/fnbeh.2022.1074682.
[22] K. Supekar, J. Kochalka, M. Schaer, H. Wakeman, S. Qin, A. Padmanabhan, V. Menon, Deficits in mesolimbic reward pathway underlie social interaction impairments in children with autism, Brain A J. Neurol. 141 (2018) 2795–2805, https://doi.org/10.1093/brain/awy191.
[23] M.V. Fuccillo, Striatal Circuits as a Common Node for Autism Pathophysiology, Front. Neurosci. 10 (2016) 27, https://doi.org/10.3389/fnins.2016.00027.
[24] D. Pfaff, H. Barbas, Mechanisms for the Approach/Avoidance Decision Applied to Autism, Trends Neurosci. 42 (2019) 448–457, https://doi.org/10.1016/j.tins.2019.05.002.
[25] J.-J. Soghomonian, The cortico-striatal circuitry in autism-spectrum disorders: a balancing act, Front. Cell. Neurosci. 17 (2024) 1329095, https://doi.org/10.3389/fncel.2023.1329095.
[26] F. Mannella, K. Gurney, G. Baldassarre, The nucleus accumbens as a nexus between values and goals in goal-directed behavior: a review and a new hypothesis, Front. Behav. Neurosci. 7 (2013) 135, https://doi.org/10.3389/fnbeh.2013.00135.
[27] M.D. Scofield, J.A. Heinsbroek, C.D. Gipson, Y.M. Kupchik, S. Spencer, A. C. Smith, D. Roberts-Wolfe, P.W. Kalivas, The Nucleus Accumbens: Mechanisms of Addiction across Drug Classes Reflect the Importance of Glutamate Homeostasis, Pharmacol. Rev. 68 (2016) 816–871, https://doi.org/10.1124/pr.116.012484.
[28] T.C. Francis, M.K. Lobo, Emerging Role for Nucleus Accumbens Medium Spiny Neuron Subtypes in Depression, Biol. Psychiatry 81 (2017) 645–653, https://doi.org/10.1016/j.biopsych.2016.09.007.
[29] S.B. Floresco, The nucleus accumbens: an interface between cognition, emotion, and action, Annu. Rev. Psychol. 66 (2015) 25–52, https://doi.org/10.1146/annurev-psych-010213-115159.
[30] P.E. Rothwell, M.V. Fuccillo, S. Maxeiner, S.J. Hayton, O. Gokce, B.K. Lim, S. C. Fowler, R.C. Malenka, T.C. Sudhof, Autism-associated neuroligin-3 mutations commonly impair striatal circuits to boost repetitive behaviors, Cell 158 (2014) 198–212, https://doi.org/10.1016/j.cell.2014.04.045.
[31] J. Le Merrer, B. Detraux, J. Gandia, A. De Groote, M. Fonteneau, A. de Kerchove d'Exaerde, J.A.J. Becker, Balance Between Projecting Neuronal Populations of the Nucleus Accumbens Controls Social Behavior in Mice, Biol. Psychiatry 95 (2024) 123–135, https://doi.org/10.1016/j.biopsych.2023.05.008.
[32] P. Zhao, X. Chen, A. Bellafard, A. Murugesan, J. Quan, D. Aharoni, P. Golshani, Cell-type-specific disruption of nucleus accumbens social representations in a mouse model of autism, 00616–1, Neuron S0896-6273 (26) (2026), https://doi.org/10.1016/j.neuron.2026.08.007.
[33] C. Soares-Cunha, N.A.P. de Vasconcelos, B. Coimbra, A.V. Domingues, J.M. Silva, E. Loureiro-Campos, R. Gaspar, I. Sotiropoulos, N. Sousa, A.J. Rodrigues, Nucleus accumbens medium spiny neurons subtypes signal both reward and aversion, Mol. Psychiatry 25 (2020) 3241–3255, https://doi.org/10.1038/s41380-019-0484-3.
[34] T.C. Francis, R. Chandra, D.M. Friend, E. Finkel, G. Dayrit, J. Miranda, J. M. Brooks, S.D. Iniguez, P. O'Donnell, A. Kravitz, M.K. Lobo, Nucleus accumbens medium spiny neuron subtypes mediate depression-related outcomes to social defeat stress, Biol. Psychiatry 77 (2015) 212–222, https://doi.org/10.1016/j.biopsych.2014.07.021.
[35] L.A. Gunaydin, L. Grosenick, J.C. Finkelstein, I.V. Kauvar, L.E. Fenno, A. Adhikari, S. Lammel, J.J. Mirzabekov, R.D. Airan, K.A. Zalocusky, K.M. Tye, P. Anikeeva, R.C. Malenka, K. Deisseroth, Natural neural projection dynamics underlying social behavior, Cell 157 (2014) 1535–1551, https://doi.org/10.1016/j.cell.2014.05.017.
[36] L. Zhang, Y. Qu, L.J. Young, W. Hou, L. Liu, J. Liu, Y. Wang, L. Li, X. Guo, Y. Li, C. Huang, Z. Lv, Y.-T. Li, R. Jia, T. Lian, H. Feng, H. Qiao, Z. He, F.-D. Tai, Different roles of D1/D2 medium spiny neurons in the nucleus accumbens in pair bond formation of male mandarin voles, Elife 13 (2025) RP100292, https://doi.org/10.7554/eLife.100292.
[37] Q. Shan, Y. Hu, S. Chen, Y. Tian, Nucleus accumbens dichotomically controls social dominance in male mice, Neuropsychopharmacol 47 (2022) 776–787, https://doi.org/10.1038/s41386-021-01220-1.
[38] K.M. Jung, M. Sepers, C.M. Henstridge, O. Lassalle, D. Neuhofer, H. Martin, M. Ginger, A. Frick, N.V. DiPatrizio, K. Mackie, I. Katona, D. Piomelli, O. J. Manzoni, Uncoupling of the endocannabinoid signalling complex in a mouse model of fragile X syndrome, Nat. Commun. 3 (2012) 1080, https://doi.org/10.1038/ncomms2045.
[39] D. Neuhofer, C.M. Henstridge, B. Dudok, M. Sepers, O. Lassalle, I. Katona, O. J. Manzoni, Functional and structural deficits at accumbens synapses in a mouse model of Fragile X, Front. Cell. Neurosci. 9 (2015) 100, https://doi.org/10.3389/fncel.2015.00100.
[40] G. Giua, O. Lassalle, L. Makrini-Maleville, E. Valjent, P. Chavis, O.J.J. Manzoni, Investigating cell-specific effects of FMRP deficiency on spiny projection neurons in a mouse model of Fragile X syndrome, Front. Cell. Neurosci. 17 (2023) 1146647, https://doi.org/10.3389/fncel.2023.1146647.
[41] G. Giua, J. Pereira-Silva, A. Caceres-Rodriguez, O. Lassalle, P. Chavis, O. J. Manzoni, Cell- and Pathway-Specific Disruptions in the Accumbens of Fragile X Mouse, J. Neurosci. 44 (2024) e1587232024, https://doi.org/10.1523/JNEUROSCI.1587-23.2024.
[42] J.A.J. Becker, L.P. Pellissier, Y. Corde, T. Laboute, A. Leaute, J. Gandia, J. Le Merrer, Facilitating mGluR4 activity reverses the long-term deleterious consequences of chronic morphine exposure in male mice, Neuropsychopharmacology 46 (2021) 1373–1385, https://doi.org/10.1038/s41386-020-00927-x.
[43] M. Amalric, S. Lopez, C. Goudet, G. Fisone, G. Battaglia, F. Nicoletti, J.P. Pin, F. C. Acher, Group III and subtype 4 metabotropic glutamate receptor agonists: discovery and pathophysiological applications in Parkinson's disease, Neuropharmacology 66 (2013) 53–64, https://doi.org/10.1016/j.neuropharm.2012.05.026.
[44] C. Corti, L. Aldegheri, P. Somogyi, F. Ferraguti, Distribution and synaptic localisation of the metabotropic glutamate receptor 4 (mGluR4) in the rodent CNS, Neuroscience 110 (2002) 403–420.
[45] S.R. Bradley, D.G. Standaert, K.J. Rhodes, H.D. Rees, C.M. Testa, A.I. Levey, P. J. Conn, Immunohistochemical localization of subtype 4a metabotropic glutamate receptors in the rat and mouse basal ganglia, J. Comp. Neurol. 407 (1999) 33–46.
[46] C.M. Niswender, K.A. Johnson, C.D. Weaver, C.K. Jones, Z. Xiang, Q. Luo, A. L. Rodriguez, J.E. Marlo, T. de Paulis, A.D. Thompson, E.L. Days, T. Nalywajko, C. A. Austin, M.B. Williams, J.E. Ayala, R. Williams, C.W. Lindsley, P.J. Conn, Discovery, characterization, and antiparkinsonian effect of novel positive allosteric modulators of metabotropic glutamate receptor 4, Mol. Pharmacol. 74 (2008) 1345–1358, https://doi.org/10.1124/mol.108.049551.
[47] D. Charvin, T. Di Paolo, E. Bezard, L. Gregoire, A. Takano, G. Duvey, E. Pioli, C. Halldin, R. Medori, F. Conquet, An mGlu4-Positive Allosteric Modulator Alleviates Parkinsonism in Primates, Mov. Disord. 33 (2018) 1619–1631, https://doi.org/10.1002/mds.27462.
[48] O. Valenti, M.J. Marino, M. Wittmann, E. Lis, A.G. DiLella, G.G. Kinney, P. J. Conn, Group III metabotropic glutamate receptor-mediated modulation of the striatopallidal synapse, J. Neurosci. 23 (2003) 7218–7226, https://doi.org/10.1523/JNEUROSCI.23-18-07218.2003.
[49] P. Svenningsson, C. Le Moine, G. Fisone, B.B. Fredholm, Distribution, biochemistry and function of striatal adenosine A2A receptors, Prog. Neurobiol. 59 (1999) 355–396, https://doi.org/10.1016/s0301-0082(99)00011-8.

[50] M. Ochi, K. Koga, M. Kurokawa, H. Kase, J. Nakamura, Y. Kuwana, Systemic administration of adenosine A(2A) receptor antagonist reverses increased GABA release in the globus pallidus of unilateral 6-hydroxydopamine-lesioned rats: a microdialysis study, Neuroscience 100 (2000) 53–62, https://doi.org/10.1016/s0306-4522(00)00250-5.
[51] R. Martin, A.S. Suarez-Pinilla, N. Garcia-Font, M.L. Laguna-Luque, J.C. Lopez-Ramos, M.J. Oset-Gasque, A. Gruart, J.M. Delgado-Garcia, M. Torres, J. Sanchez-Prieto, The activation of mGluR4 rescues parallel fiber synaptic transmission and LTP, motor learning and social behavior in a mouse model of Fragile X Syndrome, Mol. Autism 14 (2023) 14, https://doi.org/10.1186/s13229-023-00547-4.
[52] A. Ferrante, Z. Boussadia, A. Borreca, C. Mallozzi, G. Pedini, L. Pacini, A. Pezzola, M. Armida, F. Vincenzi, K. Varani, C. Bagni, P. Popoli, A. Martire, Adenosine A2A receptor inhibition reduces synaptic and cognitive hippocampal alterations in Fmr1 KO mice, Transl. Psychiatry 11 (2021) 112, https://doi.org/10.1038/s41398-021-01238-5.
[53] J. Shimada, N. Koike, H. Nonaka, S. Shiozaki, K. Yanagawa, T. Kanda, H. Kobayashi, M. Ichimura, J. Nakamura, H. Kase, F. Suzuki, Adenosine A2A antagonists with potent anti-cataleptic activity, Bioorg. & Med. Chem. Lett. 7 (1997) 2349–2352, https://doi.org/10.1016/S0960-894X(97)00440-X.
[54] R. Grondin, P.J. Bédard, A.Hadj Tahar, L. Grégoire, A. Mori, H. Kase, Antiparkinsonian effect of a new selective adenosine A2A receptor antagonist in MPTP-treated monkeys, Neurology 52 (1999) 1673–1677, https://doi.org/10.1212/wnl.52.8.1673.
[55] C. Goudet, B. Vilar, T. Courtiol, T. Deltheil, T. Bessiron, I. Brabet, N. Oueslati, D. Rigault, H.O. Bertrand, H. McLean, H. Daniel, M. Amalric, F. Acher, J.P. Pin, A novel selective metabotropic glutamate receptor 4 agonist reveals new possibilities for developing subtype selective ligands with therapeutic potential, Faseb J. 26 (2012) 1682–1693, https://doi.org/10.1096/fj.11-195941.
[56] E. Le Poul, C. Boléa, F. Girard, S. Poli, D. Charvin, B. Campo, J. Bortoli, A. Bessif, B. Luo, A.J. Koser, L.M. Hodge, K.M. Smith, A.G. DiLella, N. Liverton, F. Hess, S. E. Browne, I.J. Reynolds, A potent and selective metabotropic glutamate receptor 4 positive allosteric modulator improves movement in rodent models of Parkinson's disease, J. Pharmacol. Exp. Ther. 343 (2012) 167–177, https://doi.org/10.1124/jpet.112.196063.
[57] N. Percie du Sert, V. Hurst, A. Ahluwalia, S. Alam, M.T. Avey, M. Baker, W. J. Browne, A. Clark, I.C. Cuthill, U. Dirnagl, M. Emerson, P. Garner, S.T. Holgate, D.W. Howells, N.A. Karp, S.E. Lazic, K. Lidster, C.J. MacCallum, M. Macleod, E. J. Pearl, O.H. Petersen, F. Rawle, P. Reynolds, K. Rooney, E.S. Sena, S. D. Silberberg, T. Steckler, H. Würbel, The ARRIVE guidelines 2.0: Updated guidelines for reporting animal research, BMC Vet. Res. 16 (2020) 242, https://doi.org/10.1186/s12917-020-02451-y.
[58] C.N. Pujol, L.P. Pellissier, C. Clément, J.A.J. Becker, J. Le Merrer, Back-translating behavioral intervention for autism spectrum disorders to mice with blunted reward restores social abilities, Transl. Psychiatry 8 (2018) 197, https://doi.org/10.1038/s41398-018-0247-y.
[59] F. Acher, J.-P. Pin, C. Goudet, A. Eschalier, J. Busserolles, D. Rigault, I. Lemasson, S. Cesarini, B. Commare, Hypophosphorous acid derivatives having antihyperalgic activity and biological applications thereof, WO2012156931A1 (2012).
[60] S. Pittolo, X. Gómez-Santacana, K. Eckelt, X. Rovira, J. Dalton, C. Goudet, J.-P. Pin, A. Llobet, J. Giraldo, A. Llebaria, P. Gorostiza, An allosteric modulator to control endogenous G protein-coupled receptors with light, Nat. Chem. Biol. 10 (2014) 813–815, https://doi.org/10.1038/nchembio.1612.
[61] C. Goudet, F. Gaven, J. Kniazeff, C. Vol, J. Liu, M. Cohen-Gonsaud, F. Acher, L. Prézeau, J.P. Pin, Heptahelical domain of metabotropic glutamate receptor 5 behaves like rhodopsin-like receptors, Proc. Natl. Acad. Sci. USA 101 (2004) 378–383, https://doi.org/10.1073/pnas.0304699101.
[62] D. Eilam, H. Szechtman, Biphasic effect of D-2 agonist quinpirole on locomotion and movements, Eur. J. Pharmacol. 161 (1989) 151–157, https://doi.org/10.1016/0014-2999(89)90837-6.
[63] H.S. Bateup, E. Santini, W. Shen, S. Birnbaum, E. Valjent, D.J. Surmeier, G. Fisone, E.J. Nestler, P. Greengard, Distinct subclasses of medium spiny neurons differentially regulate striatal motor behaviors, Proc. Natl. Acad. Sci. USA 107 (2010) 14845–14850, https://doi.org/10.1073/pnas.1009874107.
[64] H. Sun, H. Monenschein, H.H. Schiffer, H.A. Reichard, S. Kikuchi, M. Hopkins, T. K. Macklin, S. Hitchcock, M. Adams, J. Green, J. Brown, S.T. Murphy, N. Kaushal, D.R. Collia, S. Moore, W.J. Ray, N.M. English, M.B.L. Carlton, N.L. Brice, First-Time Disclosure of CVN424, a Potent and Selective GPR6 Inverse Agonist for the Treatment of Parkinson's Disease: Discovery, Pharmacological Validation, and Identification of a Clinical Candidate, J. Med. Chem. 64 (2021) 9875–9890, https://doi.org/10.1021/acs.jmedchem.0c02081.
[65] Y. Katayama, M. Nishiyama, H. Shoji, Y. Ohkawa, A. Kawamura, T. Sato, M. Suyama, T. Takumi, T. Miyakawa, K.I. Nakayama, CHD8 haploinsufficiency results in autistic-like phenotypes in mice, Nature 537 (2016) 675–679, https://doi.org/10.1038/nature19357.
[66] N. Matsuo, K. Tanda, K. Nakanishi, N. Yamasaki, K. Toyama, K. Takao, H. Takeshima, T. Miyakawa, Comprehensive behavioral phenotyping of ryanodine receptor type 3 (RyR3) knockout mice: decreased social contact duration in two social interaction tests, Front. Behav. Neurosci. 3 (2009) 3, https://doi.org/10.3389/neuro.08.003.2009.
[67] J.L. Silverman, M. Yang, C. Lord, J.N. Crawley, Behavioural phenotyping assays for mouse models of autism, Nat. Rev. Neurosci. 11 (2010) 490–502, https://doi.org/10.1038/nrn2851.
[68] S.S. Moy, N.V. Riddick, V.D. Nikolova, B.L. Teng, K.L. Agster, R.J. Nonneman, N. B. Young, L.K. Baker, J.J. Nadler, J.W. Bodfish, Repetitive behavior profile and supersensitivity to amphetamine in the C58/J mouse model of autism, Behav. Brain Res. 259 (2014) 200–214, https://doi.org/10.1016/j.bbr.2013.10.052.
[69] A. Thomas, A. Burant, N. Bui, D. Graham, L.A. Yuva-Paylor, R. Paylor, Marble burying reflects a repetitive and perseverative behavior more than novelty-induced anxiety, Psychopharmacol. (Berl.) 204 (2009) 361–373, https://doi.org/10.1007/s00213-009-1466-y.
[70] D. Delotterie, G. Ruiz, J. Brocard, A. Schweitzer, C. Roucard, Y. Roche, M. F. Suaud-Chagny, K. Bressand, A. Andrieux, Chronic administration of atypical antipsychotics improves behavioral and synaptic defects of STOP null mice, Psychopharmacol. (Berl.) 208 (2010) 131–141, https://doi.org/10.1007/s00213-009-1712-3.
[71] N. Le Marec, K. Ethier, P.P. Rompre, R. Godbout, Involvement of the medial prefrontal cortex in two alternation tasks using different environments, Brain Cogn. 48 (2002) 432–436.
[72] M. Zhou, H. Rebholz, C. Brocia, J.L. Warner-Schmidt, A.A. Fienberg, A.C. Nairn, P. Greengard, M. Flajolet, Forebrain overexpression of CK1delta leads to down-regulation of dopamine receptors and altered locomotor activity reminiscent of ADHD, Proc. Natl. Acad. Sci. USA 107 (2010) 4401–4406, https://doi.org/10.1073/pnas.0915173107.
[73] P. Laurent, J.A. Becker, O. Valverde, C. Ledent, A. de Kerchove d'Exaerde, S. N. Schiffmann, R. Maldonado, G. Vassart, M. Parmentier, The prolactin-releasing peptide antagonizes the opioid system through its receptor GPR10, Nat. Neurosci. 8 (2005) 1735–1741, https://doi.org/10.1038/nn1585.
[74] A. Ennaceur, N. Neave, J.P. Aggleton, Spontaneous object recognition and object location memory in rats: the effects of lesions in the cingulate cortices, the medial prefrontal cortex, the cingulum bundle and the fornix, Exp. Brain Res. 113 (1997) 509–519.
[75] C. Derieux, A. Leaute, A. Brugoux, D. Jaccaz, C. Terrier, J.P. Pin, J. Kniazeff, J. Le Merrer, J.A.J. Becker, Chronic sodium bromide treatment relieves autistic-like behavioral deficits in three mouse models of autism, Neuropsychopharmacology 47 (2022) 1680–1692, https://doi.org/10.1038/s41386-022-01317-1.
[76] S. Pietropaolo, A. Guilleminot, B. Martin, F.R. D'Amato, W.E. Crusio, Genetic-background modulation of core and variable autistic-like symptoms in Fmr1 knock-out mice, PLoS. One 6 (2011) e17073, https://doi.org/10.1371/journal.pone.0017073.
[77] C.M. Spencer, O. Alekseyenko, E. Serysheva, L.A. Yuva-Paylor, R. Paylor, Altered anxiety-related and social behaviors in the Fmr1 knockout mouse model of fragile X syndrome, Genes. Brain Behav. 4 (2005) 420–430, https://doi.org/10.1111/j.1601-183X.2005.00123.x.
[78] L.J. Martin, S.J. Poulson, E. Mannan, S. Sivaselvachandran, M. Cho, F. Setak, C. Chan, Altered nociceptive behavior and emotional contagion of pain in mouse models of autism, Genes. Brain Behav. 21 (2022) e12778, https://doi.org/10.1111/gbb.12778.
[79] A. Borreca, M. De Luca, A. Ferrante, Z. Boussadia, A. Pignataro, A. Martire, M. Ammassari-Teule, Fmr1-KO mice failure to detect object novelty associates with a post-test decrease of structural and synaptic plasticity upstream of the hippocampus, Sci. Rep. 13 (2023) 755, https://doi.org/10.1038/s41598-023-27991-9.
[80] R. Klar, A.G. Walker, D. Ghose, B.A. Grueter, D.W. Engers, C.R. Hopkins, C. W. Lindsley, Z. Xiang, P.J. Conn, C.M. Niswender, Activation of Metabotropic Glutamate Receptor 7 Is Required for Induction of Long-Term Potentiation at SC-CA1 Synapses in the Hippocampus, J. Neurosci. 35 (2015) 7600–7615, https://doi.org/10.1523/JNEUROSCI.4543-14.2015.
[81] C. Zussy, X. Gomez-Santacana, X. Rovira, D. De Bundel, S. Ferrazzo, D. Bosch, D. Asede, F. Malhaire, F. Acher, J. Giraldo, E. Valjent, I. Ehrlich, F. Ferraguti, J. P. Pin, A. Llebaria, C. Goudet, Dynamic modulation of inflammatory pain-related affective and sensory symptoms by optical control of amygdala metabotropic glutamate receptor 4, Mol. Psychiatry 23 (2018) 509–520, https://doi.org/10.1038/mp.2016.223.
[82] H. Ohishi, C. Akazawa, R. Shigemoto, S. Nakanishi, N. Mizuno, Distributions of the mRNAs for L-2-amino-4-phosphonobutyrate-sensitive metabotropic glutamate receptors, mGluR4 and mGluR7, in the rat brain, J. Comp. Neurol. 360 (1995) 555–570, https://doi.org/10.1002/cne.903600402.
[83] C. Soares-Cunha, J.A. Heinsbroek, Ventral pallidal regulation of motivated behaviors and reinforcement, Front. Neural Circuits 17 (2023) 1086053, https://doi.org/10.3389/fncir.2023.1086053.
[84] V. Pereira, J.A. Arias, A. Llebaria, C. Goudet, Photopharmacological manipulation of amygdala metabotropic glutamate receptor mGlu4 alleviates neuropathic pain, Pharmacol. Res. 187 (2023) 106602, https://doi.org/10.1016/j.phrs.2022.106602.
[85] O. Gokce, G. Stanley, B. Treutlein, N.F. Neff, G.J. Camp, R.C. Malenka, P. E. Rothwell, M.V. Fuccillo, T.C. Südhof, S.R. Quake, Cellular Taxonomy of the Mouse Striatum as Revealed by Single-Cell RNA-Seq, Cell. Rep. 16 (2016) 1126–1137, https://doi.org/10.1016/j.celrep.2016.06.059.
[86] A.A. Caudy, M. Myers, G.J. Hannon, S.M. Hammond, Fragile X-related protein and VIG associate with the RNA interference machinery, Genes. Dev. 16 (2002) 2491–2496, https://doi.org/10.1101/gad.1025202.
[87] K.E. Reynolds, V. Krasovska, A.L. Scott, Converging purinergic and immune signaling pathways drive IL-6 secretion by Fragile X cortical astrocytes via STAT3, J. Neuroimmunol. 361 (2021) 577745, https://doi.org/10.1016/j.jneuroim.2021.577745.
[88] Y. Luan, H. Zhang, N. Ma, Y. Zhang, Z. Xu, W. Zhang, X. Zhang, Y. Liu, HK2 drives synaptic dysfunction in fragile X syndrome via epigenetic regulation of H3K18 lactylation, Front. Pharmacol. 17 (2026) 1903604, https://doi.org/10.3389/fphar.2026.1903604.

[89] M. Pardo, Y. Cheng, D. Velmeshev, M. Magistri, H. Eldar-Finkelman, A. Martinez, M.A. Faghihi, R.S. Jope, E. Beurel, Intranasal siRNA administration reveals IGF2 deficiency contributes to impaired cognition in Fragile X syndrome mice, JCI Insight 2 (2017) e91782, https://doi.org/10.1172/jci.insight.91782.
[90] A. Ishizuka, M.C. Siomi, H. Siomi, A Drosophila fragile X protein interacts with components of RNAi and ribosomal proteins, Genes. Dev. 16 (2002) 2497–2508, https://doi.org/10.1101/gad.1022002.
[91] P. Jin, D.C. Zarnescu, S. Ceman, M. Nakamoto, J. Mowrey, T.A. Jongens, D. L. Nelson, K. Moses, S.T. Warren, Biochemical and genetic interaction between the fragile X mental retardation protein and the microRNA pathway, Nat. Neurosci. 7 (2004) 113–117, https://doi.org/10.1038/nn1174.
[92] I. Plante, L. Davidovic, D.L. Ouellet, L.-A. Gobeil, S. Tremblay, E.W. Khandjian, P. Provost, Dicer-derived microRNAs are utilized by the fragile X mental retardation protein for assembly on target RNAs, J. Biomed. Biotechnol. 2006 (2006) 64347, https://doi.org/10.1155/JBB/2006/64347.
[93] M.-C. Didiot, M. Subramanian, E. Flatter, J.-L. Mandel, H. Moine, Cells lacking the fragile X mental retardation protein (FMRP) have normal RISC activity but exhibit altered stress granule assembly, Mol. Biol. Cell. 20 (2009) 428–437, https://doi.org/10.1091/mbc.e08-07-0737.
[94] N. Kaul, S.J. Pradhan, N.G. Boin, M.M. Mason, J. Rosales, E.L. Starke, E. C. Wilkinson, E.G. Chapman, S.A. Barbee, FMRP cooperates with miRISC components to repress translation and regulate neurite morphogenesis in Drosophila, RNA Biol. 21 (2024) 11–22, https://doi.org/10.1080/15476286.2024.2392304.
[95] V. Menon, J. Leroux, C.D. White, A.L. Reiss, Frontostriatal deficits in fragile X syndrome: relation to FMR1 gene expression, Proc. Natl. Acad. Sci. USA 101 (2004) 3615–3620, https://doi.org/10.1073/pnas.0304544101.
[96] D.X. Peng, R.G. Kelley, E.-M. Quintin, M. Raman, P.M. Thompson, A.L. Reiss, Cognitive and behavioral correlates of caudate subregion shape variation in fragile X syndrome, Hum. Brain Mapp. 35 (2014) 2861–2868, https://doi.org/10.1002/hbm.22376.
[97] D. Centonze, S. Rossi, V. Mercaldo, I. Napoli, M.T. Ciotti, V. De Chiara, A. Musella, C. Prosperetti, P. Calabresi, G. Bernardi, C. Bagni, Abnormal striatal GABA transmission in the mouse model for the fragile X syndrome, Biol. Psychiatry 63 (2008) 963–973, https://doi.org/10.1016/j.biopsych.2007.09.008.
[98] V. Mercaldo, B. Vidimova, D. Gastaldo, E. Fernández, A.C. Lo, G. Cencelli, G. Pedini, S. De Rubeis, F. Longo, E. Klann, A.B. Smit, S.G.N. Grant, T. Achsel, C. Bagni, Altered striatal actin dynamics drives behavioral inflexibility in a mouse model of fragile X syndrome, Neuron 111 (2023) 1760–1775.e8, https://doi.org/10.1016/j.neuron.2023.03.008.
[99] J.L. Huebschman, C.A. Monterrey, D.M. Foster, C.C. Omoregie, A.E. Cakir, A. Sevilla-Gutierrez, E.C. Chow, A. Essoh, Y. Guo, L.N. Smith, The role of the dorsal striatum in a mouse model for fragile X syndrome: Behavioral and dendritic spine assessment, Brain Res. 1795 (2022) 148060, https://doi.org/10.1016/j.brainres.2022.148060.
[100] F. Longo, S. Aryal, P.G. Anastasiades, M. Maltese, C. Baimel, F. Albanese, J. Tabor, J.D. Zhu, M.M. Oliveira, D. Gastaldo, C. Bagni, E. Santini, N.X. Tritsch, A. G. Carter, E. Klann, Cell-type-specific disruption of cortico-striatal circuitry drives repetitive patterns of behavior in fragile X syndrome model mice, Cell. Rep. 42 (2023) 112901, https://doi.org/10.1016/j.celrep.2023.112901.
[101] J. Le Merrer, X. Rezai, G. Scherrer, J.A.J. Becker, B.L. Kieffer, Impaired hippocampus-dependent and facilitated striatum-dependent behaviors in mice lacking the δ opioid receptor, Neuropsychopharmacology 38 (2013) 1050–1059, https://doi.org/10.1038/npp.2013.1.
[102] A. Tammimäki, K. Pietilä, H. Raattamaa, L. Ahtee, Effect of quinpirole on striatal dopamine release and locomotor activity in nicotine-treated mice, Eur. J. Pharmacol. 531 (2006) 118–125, https://doi.org/10.1016/j.ejphar.2005.12.027.
[103] E.P. Bello, Y. Mateo, D.M. Gelman, D. Noaín, J.H. Shin, M.J. Low, V.A. Alvarez, D. M. Lovinger, M. Rubinstein, Cocaine supersensitivity and enhanced motivation for reward in mice lacking dopamine D2 autoreceptors, Nat. Neurosci. 14 (2011) 1033–1038, https://doi.org/10.1038/nn.2862.
[104] A. Anzalone, J.E. Lizardi-Ortiz, M. Ramos, C. De Mei, F.W. Hopf, C. Iaccarino, B. Halbout, J. Jacobsen, C. Kinoshita, M. Welter, M.G. Caron, A. Bonci, D. Sulzer, E. Borrelli, Dual Control of Dopamine Synthesis and Release by Presynaptic and Postsynaptic Dopamine D2 Receptors, J. Neurosci. 32 (2012) 9023–9034, https://doi.org/10.1523/JNEUROSCI.0918-12.2012.
[105] S. Chhabra, L. Nardi, P. Leukel, C.J. Sommer, M.J. Schmeisser, Striatal increase of dopamine receptor 2 density in idiopathic and syndromic mouse models of autism spectrum disorder, Front. Psychiatry 14 (2023) 1110525, https://doi.org/10.3389/fpsyt.2023.1110525.
[106] E.F. Gallo, M.C. Salling, B. Feng, J.A. Morón, N.L. Harrison, J.A. Javitch, C. Kellendonk, Upregulation of dopamine D2 receptors in the nucleus accumbens indirect pathway increases locomotion but does not reduce alcohol consumption, Neuropsychopharmacology 40 (2015) 1609–1618, https://doi.org/10.1038/npp.2015.11.
[107] B. Costall, D.H. Fortune, R.J. Naylor, The induction of catalepsy and hyperactivity by morphine administered directly into the nucleus accumbens of rats, Eur. J. Pharmacol. 49 (1978) 49–64, https://doi.org/10.1016/0014-2999(78)90221-2.
[108] M. Winkler, U. Havemann, K. Kuschinsky, Unilateral injection of morphine into the nucleus accumbens induces akinesia and catalepsy, but no spontaneous muscular rigidity in rats, Naunyn Schmiede Arch. Pharmacol. 318 (1982) 143–147, https://doi.org/10.1007/BF00500473.
[109] R. Chen, T.R. Blosser, M.N. Djekidel, J. Hao, A. Bhattacherjee, W. Chen, L. M. Tuesta, X. Zhuang, Y. Zhang, Decoding molecular and cellular heterogeneity of mouse nucleus accumbens, Nat. Neurosci. 24 (2021) 1757–1771, https://doi.org/10.1038/s41593-021-00938-x.
[110] T. Kanda, S. Shiozaki, J. Shimada, F. Suzuki, J. Nakamura, KF17837: A novel selective adenosine A2A receptor antagonist with anticataleptic activity, Eur. J. Pharmacol. 256 (1994) 263–268, https://doi.org/10.1016/0014-2999(94)90551-7.
[111] M.R. Zarrindast, F. Iraie, M.R. Heidari, M. Mohagheghi-Badi, Effect of adenosine receptor agonists and antagonists on morphine-induced catalepsy in mice, Eur. J. Pharmacol. 338 (1997) 11–16, https://doi.org/10.1016/s0014-2999(97)01221-1.
[112] Y. Zhang, J. Gao, N. Li, P. Xu, S. Qu, J. Cheng, M. Wang, X. Li, Y. Song, F. Xiao, X. Yang, J. Liu, H. Hong, R. Mu, X. Li, Y. Wang, H. Xu, Y. Xie, T. Gao, G. Wang, J. Aa, Targeting cAMP in D1-MSNs in the nucleus accumbens, a new rapid antidepressant strategy, Acta Pharm. Sin. B 14 (2024) 667–681, https://doi.org/10.1016/j.apsb.2023.12.005.
[113] L. Iskhakova, Y. Smith, mGluR4-containing corticostriatal terminals: synaptic interactions with direct and indirect pathway neurons in mice, Brain Struct. Funct. 221 (2016) 4589–4599, https://doi.org/10.1007/s00429-016-1187-z.
[114] J.P. Aggleton, A.J.D. Nelson, Distributed interactive brain circuits for object-in-place memory: A place for time? Brain Neurosci. Adv. 4 (2020) 2398212820933471 https://doi.org/10.1177/2398212820933471.
[115] B. Vilar, J. Busserolles, B. Ling, S. Laffray, L. Ulmann, F. Malhaire, E. Chapuy, Y. Aissouni, M. Etienne, E. Bourinet, F. Acher, J.P. Pin, A. Eschalier, C. Goudet, Alleviating pain hypersensitivity through activation of type 4 metabotropic glutamate receptor, J. Neurosci. 33 (2013) 18951–18965, https://doi.org/10.1523/JNEUROSCI.1221-13.2013.
[116] V. Kumar, K.Y. Lee, A. Acharya, M.S. Babik, C.A. Christian-Hinman, J.S. Rhodes, N.-P. Tsai, mGluR7 allosteric modulator AMN082 corrects protein synthesis and pathological phenotypes in FXS, EMBO Mol. Med. 16 (2024) 506–522, https://doi.org/10.1038/s44321-024-00038-w.
[117] R.G. Gogliotti, R.K. Senter, N.M. Fisher, J. Adams, R. Zamorano, A.G. Walker, A. L. Blobaum, D.W. Engers, C.R. Hopkins, J.S. Daniels, C.K. Jones, C.W. Lindsley, Z. Xiang, P.J. Conn, C.M. Niswender, mGlu7 potentiation rescues cognitive, social, and respiratory phenotypes in a mouse model of Rett syndrome, Sci. Transl. Med. 9 (2017), https://doi.org/10.1126/scitranslmed.aai7459.
[118] N. Jalan-Sakrikar, J.R. Field, R. Klar, M.E. Mattmann, K.J. Gregory, R. Zamorano, D.W. Engers, S.R. Bollinger, C.D. Weaver, E.L. Days, L.M. Lewis, T.J. Utley, M. Hurtado, D. Rigault, F. Acher, A.G. Walker, B.J. Melancon, M.R. Wood, C. W. Lindsley, P.J. Conn, Z. Xiang, C.R. Hopkins, C.M. Niswender, Identification of positive allosteric modulators VU0155094 (ML397) and VU0422288 (ML396) reveals new insights into the biology of metabotropic glutamate receptor 7, ACS Chem. Neurosci. 5 (2014) 1221–1237, https://doi.org/10.1021/cn500153z.
[119] J.J.G. Geurts, G. Wolswijk, L. Bö, S. Redeker, M. Ramkema, D. Troost, E. Aronica, Expression patterns of Group III metabotropic glutamate receptors mGluR4 and mGluR8 in multiple sclerosis lesions, J. Neuroimmunol. 158 (2005) 182–190, https://doi.org/10.1016/j.jneuroim.2004.08.012.
[120] S.F. Spampinato, S. Merlo, M. Chisari, F. Nicoletti, M.A. Sortino, Glial metabotropic glutamate receptor-4 increases maturation and survival of oligodendrocytes, Front. Cell. Neurosci. 8 (2015) 462, https://doi.org/10.3389/fncel.2014.00462.
[121] E. Kuramoto, F. Fujiyama, T. Unzai, K. Nakamura, H. Hioki, T. Furuta, R. Shigemoto, F. Ferraguti, T. Kaneko, Metabotropic glutamate receptor 4-immunopositive terminals of medium-sized spiny neurons selectively form synapses with cholinergic interneurons in the rat neostriatum, J. Comp. Neurol. 500 (2007) 908–922, https://doi.org/10.1002/cne.21216.
[122] J.B. Ding, J.N. Guzman, J.D. Peterson, J.A. Goldberg, D.J. Surmeier, Thalamic gating of corticostriatal signaling by cholinergic interneurons, Neuron 67 (2010) 294–307, https://doi.org/10.1016/j.neuron.2010.06.017.
[123] B.S. Muntean, M.T. Dao, K.A. Martemyanov, Allostatic Changes in the cAMP System Drive Opioid-Induced Adaptation in Striatal Dopamine Signaling, Cell. Rep. 29 (2019) 946–960.e2, https://doi.org/10.1016/j.celrep.2019.09.034.
[124] J.A. Becker, D. Clesse, C. Spiegelhalter, Y. Schwab, J. Le Merrer, B.L. Kieffer, Autistic-like syndrome in mu opioid receptor null mice is relieved by facilitated mGluR4 activity, Neuropsychopharmacology 39 (2014) 2049–2060, https://doi.org/10.1038/npp.2014.59.
[125] L. Garbugino, E. Centofante, F.R. D'Amato, Early Social Enrichment Improves Social Motivation and Skills in a Monogenic Mouse Model of Autism, the Oprm1 −/− Mouse, Neural Plast. 2016 (2016) 5346161, https://doi.org/10.1155/2016/5346161.
[126] K.I. Ramírez-Armenta, H. Alatriste-León, A.K. Verma-Rodríguez, A. Llanos-Moreno, J.O. Ramírez-Jarquín, F. Tecuapetla, Optogenetic inhibition of indirect pathway neurons in the dorsomedial striatum reduces excessive grooming in Sapap3-knockout mice, Neuropsychopharmacology 47 (2022) 477–487, https://doi.org/10.1038/s41386-021-01161-9.
[127] S.C. Piantadosi, E.E. Manning, B.L. Chamberlain, J. Hyde, Z. LaPalombara, N. M. Bannon, J.L. Pierson, V.M. K Namboodiri, S.E. Ahmari, Hyperactivity of indirect pathway-projecting spiny projection neurons promotes compulsive behavior, Nat. Commun. 15 (2024) 4434, https://doi.org/10.1038/s41467-024-48331-z.
[128] T. Sippy, N.X. Tritsch, Unraveling the dynamics of dopamine release and its actions on target cells, Trends Neurosci. 46 (2023) 228–239, https://doi.org/10.1016/j.tins.2022.12.005.
[129] C. Varin, A. de Kerchove d'Exaerde, Neuronal encoding of behaviors and instrumental learning in the dorsal striatum, Trends Neurosci. 48 (2025) 77–91, https://doi.org/10.1016/j.tins.2024.11.003.
[130] L. Faget, V. Zell, E. Souter, A. McPherson, R. Ressler, N. Gutierrez-Reed, J.H. Yoo, D. Dulcis, T.S. Hnasko, Opponent control of behavioral reinforcement by

inhibitory and excitatory projections from the ventral pallidum, Nat. Commun. 9 (2018) 849, https://doi.org/10.1038/s41467-018-03125-y.
[131] M. Stephenson-Jones, C. Bravo-Rivera, S. Ahrens, A. Furlan, X. Xiao, C. Fernandes-Henriques, B. Li, Opposing contributions of GABAergic and glutamatergic ventral pallidal neurons to motivational behaviors, Neuron 105 (2020) 921–933.e5, https://doi.org/10.1016/j.neuron.2019.12.006.
[132] F. Wang, J. Zhang, Y. Yuan, M. Chen, Z. Gao, S. Zhan, C. Fan, W. Sun, J. Hu, Salience processing by glutamatergic neurons in the ventral pallidum, Sci. Bull. 65 (2020) 389–401, https://doi.org/10.1016/j.scib.2019.11.029.
[133] D. Knowland, V. Lilascharoen, C.P. Pacia, S. Shin, E.H.-J. Wang, B.K. Lim, Distinct ventral pallidal neural populations mediate separate symptoms of depression, Cell 170 (2017) 284–297.e18, https://doi.org/10.1016/j.cell.2017.06.015.